

Phenomenological Analysis of Single-Pion Photoproduction*

R. L. WALKER

California Institute of Technology, Pasadena, California 91109

(Received 29 May 1968; revised manuscript received 7 April 1969)

A phenomenological fit of the data on single-pion photoproduction is presented for laboratory photon energies up to 1.2 BeV. The analysis is made in terms of a simple model in which the photoproduction amplitude consists of three separate contributions: (1) the Born approximation with electric coupling only; (2) Breit-Wigner resonances for which the positions and widths are taken from pion-nucleon scattering data, but whose amplitudes are adjustable parameters; and (3) additional contributions in the low partial waves having $J = \frac{1}{2}, \frac{3}{2},$ and $\frac{5}{2}$. A criterion for success of the model is that these added terms, which are the principal adjustable parameters, should vary smoothly with energy. Most of the resonances found in the phase-shift analysis of pion-nucleon scattering are included in the fit. In particular, there is reasonably good evidence in the photoproduction data for a broad S -wave resonance near 1560 MeV. The analysis is carried out in terms of the helicity-amplitude formalism, which is more convenient for this purpose than the conventional representation in terms of multipole amplitudes.

I. INTRODUCTION

IN the past few years there has been a considerable improvement in our experimental knowledge of the single-pion photoproduction processes in the low-energy region below 1.5 BeV.¹ Extensive and relatively accurate cross-section data have been obtained for π^+ photoproduction and, to a lesser extent, for the production of π^0 from protons. In addition, a significant amount of data is becoming available on the polarization of recoil protons in π^0 production and on the asymmetries in photoproduction from linearly polarized photons. At the same time, there has been a revival of theoretical interest in the results of a multipole analysis because of its applications to the testing of sum rules and other relations of current theoretical importance.²⁻⁸

Also during recent years, improvements in the experimental data on pion-nucleon scattering have made it possible to carry out successful phase-shift analyses, the results of which have been both interesting and surprising.⁹ These analyses have revealed new resonances not suspected from any qualitative evidence.

It is of interest to see what effect these resonances have on the related photoproduction reactions.

A number of analyses of pion photoproduction data have recently been made. One of the first was a fitting of π^+ and π^0 data with an "isobar model" by Gourdin and Salin.¹⁰ The experimental data have been considerably augmented and improved since the time of their work, so that a new analysis is needed. A recent analysis has been carried out by Chau, Dombey, and Moorhouse,¹¹ but it covers a rather restricted energy region, and does not include the $\gamma n \rightarrow \pi^- p$ reaction.

Other work, based on dispersion relations, has been carried on over several years by Höhler, Schmidt, and their colleagues at Karlsruhe. Most of this work has concentrated on the low-energy region,¹²⁻¹⁴ but recently an extension to 1.2 BeV has been made.¹⁵ Other investigations in the low-energy region include the analysis of Donnachie and Shaw,¹⁶ and a prediction of photoproduction from pion-nucleon scattering data by means of dispersion relations, made by Berends, Donnachie, and Weaver.¹⁷

It is probably not reasonable to attempt a fit of the photoproduction data by asking a computer to search for best values of all of the parameters in an unbiased way. The difficulty is that the experimental information on photoproduction is less complete than that on pion-nucleon scattering, whereas there are approximately twice as many parameters needed to describe photoproduction within a given range of angular momentum

* Supported in part by the U. S. Atomic Energy Commission. Prepared under Contract No. AT(11-1)-68 for the San Francisco Operations Office, U. S. Atomic Energy Commission.

¹ A compilation of relevant data has been made by J. T. Beale, S. D. Ecklund, and R. L. Walker, Report No. CTSL-42, California Institute of Technology Synchrotron Laboratory, Pasadena, Calif. (unpublished). References to papers from which the data used in the present analysis have been taken will be given below, in Sec. V.

² S. Fubini, G. Furlan, and C. Rossetti, *Nuovo Cimento* **40**, 1171 (1965).

³ S. L. Adler and F. J. Gilman, *Phys. Rev.* **152**, 1460 (1966).

⁴ F. J. Gilman and H. J. Schnitzer, *Phys. Rev.* **150**, 1362 (1966).

⁵ A. Bietti, P. Di Vecchia, F. Drago, and M. L. Paciello, *Phys. Letters* **26B**, 457 (1968).

⁶ D. P. Roy and Shu-Yuan Chu, *Phys. Rev.* **171**, 1762 (1968).

⁷ R. Dolen, D. Horn, and C. Schmid, *Phys. Rev.* **166**, 1768 (1968); A. Logunov, L. D. Soloviev, and A. N. Tavkhelidze, *Phys. Letters* **24B**, 181 (1967); K. Igi and S. Matsuda, *Phys. Rev. Letters* **18**, 625 (1967).

⁸ A. Bietti, P. Di Vecchia, and F. Drago, *Nuovo Cimento* **49**, 511 (1967).

⁹ See, for example, P. Bareyre, C. Bricman, and G. Villet, *Phys. Rev.* **165**, 1730 (1968). This paper contains many references to previous experimental and theoretical work.

¹⁰ M. Gourdin and Ph. Salin, *Nuovo Cimento* **27**, 193 (1963); Ph. Salin, *ibid.* **28**, 1294 (1963).

¹¹ Y. C. Chau, N. Dombey, and R. G. Moorhouse, *Phys. Rev.* **163**, 1632 (1967).

¹² G. Höhler and W. Schmidt, *Ann. Phys. (N. Y.)* **28**, 34 (1964).

¹³ W. Schmidt, *Z. Physik* **182**, 76 (1964).

¹⁴ G. Höhler, *Ergeb. Exact. Naturw.* **39**, 55 (1965).

¹⁵ G. Schwiderski and W. Schmidt, in *Proceedings of the International Conference on Low and Intermediate Energy Electromagnetic Interactions*, Dubna, 1967 (unpublished); also, G. Schwiderski, *Technischen Hochschule Karlsruhe Report*, 1967 (unpublished).

¹⁶ A. Donnachie and G. Shaw, *Ann. Phys. (N. Y.)* **37**, 333 (1966).

¹⁷ F. A. Berends, A. Donnachie, and D. L. Weaver, *Nucl. Phys.* **B4**, 54 (1967).

states. It therefore seems necessary to impose some restrictions on the variations of the parameters. The model used to impose these limitations in the present analysis is described in the next section.

II. MODEL

We wish to determine the multipole amplitudes, or equivalent helicity amplitudes, as functions of energy. Near a resonance, the resonant amplitude is expected to vary rapidly with energy in a manner characteristic of the resonance. We shall assume that this behavior is adequately described by a Breit-Wigner function, realizing that this assumption may not be justified in view of the remarkable behavior exhibited by some of the pion-nucleon scattering amplitudes.⁹

In addition to the resonances, we shall include adjustable contributions to the partial-wave helicity amplitudes in the states of low angular momentum $J = \frac{1}{2}, \frac{3}{2}$, and, to a small extent, $J = \frac{5}{2}$. It is hoped that these added nonresonant contributions will vary smoothly with energy, and this is the criterion of success for the model. In allowing arbitrary variations in the low partial waves, we adopt the point of view that no theory at present is capable of predicting the contributions in these states of low angular momentum. It follows that the relevance to photoproduction of any particular Feynman diagram or particle exchange term can be established only through its higher partial-wave components.

One Born term, corresponding to the one-pion-exchange mechanism, contributes significantly to many higher partial waves. As is well known,¹⁸ this fact means that one must include this term explicitly in any analysis of charged pion photoproduction involving a finite number of parameters. We have included the contribution from this one-pion-exchange term together with other Born terms which make it gauge-invariant. These comprise the electric Born approximation of Sec. III 6. In the energy region under investigation, other Born diagrams contribute mainly to the low partial waves and have not been included explicitly.

In summary, the photoproduction amplitude is made up of the following three contributions: (1) the Born approximation with electric coupling, as given explicitly in Sec. III 6 (this part is the only contribution to the states of higher angular momentum); (2) resonances described by the Breit-Wigner formula of Sec. III 8; and (3) additional contributions in the states of angular momentum $J = \frac{1}{2}, \frac{3}{2}$, and, to a minor extent, $J = \frac{5}{2}$. These added contributions, together with the magnitudes of the Breit-Wigner resonances, are the parameters adjusted in making the fit.

The model adopted here is not very different from the isobar model used earlier by Gourdin and Salin,¹⁰ and it is also quite similar to the one employed in the recent work of Chau, Dombey, and Moorhouse.¹¹

The principal objective of the present analysis was to investigate photoproduction in the energy region 0.5–1.2 BeV, and most of the effort was devoted to this aim. The analysis was extended to lower energies for reasons of continuity and also to see how the same approach would work there. However, because of limitations in the data as well as in the analysis, the results below 0.5 BeV are probably not as reliable as those obtained by the use of dispersion relations. For these results, which rest on a better theoretical basis, see Refs. 12–17, and also other work referred to in these papers.

III. FORMALISM

In this section is assembled a collection of formulas used in the present analysis together with a few formulas of general interest. The conventions and units used in this work are also given here.

1. Kinematics and Units

Four-momenta of the incident photon, the outgoing pion, the initial nucleon, and the final nucleon are denoted by $k = (\mathbf{k}, k)$, $q = (\mathbf{q}, \omega)$, $p_1 = (\mathbf{p}_1, E_1)$, and $p_2 = (\mathbf{p}_2, E_2)$. Helicities of these four particles are λ_k , λ_q , λ_1 , and λ_2 , respectively. The incident photon has polarization vector ϵ , and the total energy in the c.m. system is W .

The kinematic variables s , t , and u are

$$\begin{aligned} s &= (k + p_1)^2 = W^2, \\ t &= (k - q)^2 = -2k\omega(1 - \beta_\pi \cos\theta) + m_\pi^2, \\ u &= (k - p_2)^2 = -2kE_2(1 - \beta_2 \cos\theta_2) + M_2^2. \end{aligned} \quad (1)$$

We use 1 BeV as the unit of energy and other units such that $\hbar = c = 1$. Then the unit of length is $\lambda_u = 1$ BeV⁻¹ = 1.972×10^{-14} cm, and the unit of cross section is

$$\lambda_u^2 = 1 \text{ BeV}^{-2} = 389.5 \mu\text{b}.$$

These units pertain to the “theoretical” formulas only. All numerical values quoted for amplitudes, helicity coefficients, etc., are in units $\mu\text{b}^{1/2}$.

2. Photoproduction Amplitude

We define an amplitude A , related to the S matrix by

$$S = 1 + (2\pi)^4 i \delta^4(P_f - P_i) (8\pi W N) A, \quad (2)$$

where $P_i = k + p_1$, $P_f = q + p_2$, and N is a normalization factor:

$$N = (16k\omega E_1 E_2)^{1/2}. \quad (3)$$

The spin dependence may be given by writing A as a 2×2 matrix whose columns and rows refer to initial and final nucleon spins, respectively, and whose elements depend on the photon polarization as well as on θ and W :

$$A = (A_{fi}) = \begin{pmatrix} A_{11} & A_{12} \\ A_{21} & A_{22} \end{pmatrix}. \quad (4)$$

¹⁸ M. J. Moravcsik, Phys. Rev. **104**, 1451 (1956).

The differential cross section and final nucleon polarization in direction \hat{d} are then

$$\sigma(\theta) = \frac{1}{2} \frac{q}{k} \sum_{\text{spins}} |A_{fi}|^2 = \frac{1}{2} \frac{q}{k} \text{Tr} A^\dagger A, \quad (5)$$

$$\mathbf{P} \cdot \hat{d} = -\frac{1}{2} \frac{q}{k} \frac{1}{\sigma(\theta)} \text{Tr} A^\dagger \boldsymbol{\sigma} \cdot \hat{d} A, \quad (6)$$

where these relations still refer to a given photon polarization, and the Pauli-spin matrix $\boldsymbol{\sigma}$ is in the same coordinate system used for the final-spin specification in the matrix A .

3. Helicity Amplitudes

In the center-of-momentum (c.m.) system, if we quantize initial and final spins along the directions of \mathbf{k} and \mathbf{q} , the elements of A are the *helicity amplitudes* $A_{\mu\lambda}(\theta, \phi)$, where λ and μ are the initial- and final-state helicities $\lambda = \lambda_k - \lambda_1$ and $\mu = \lambda_q - \lambda_2 = -\lambda_2$.

Since $\lambda_k = \pm 1$ for real, transverse photons, λ takes on the four values $\pm \frac{1}{2}$ and $\pm \frac{3}{2}$, any one of which specifies both λ_k and λ_1 uniquely. The eight helicity amplitudes $A_{\mu\lambda}$ are not independent, the four with $\lambda_k = -1$ being simply related to the four with $\lambda_k = +1$ by parity symmetry¹⁹:

$$A_{-\mu, -\lambda}(\theta, \phi) = -e^{i(\lambda - \mu)(\pi - 2\phi)} A_{\mu, \lambda}(\theta, \phi). \quad (7)$$

Specifically, if we let H_1, \dots, H_4 be the four helicity amplitudes with $\lambda_k = +1$, and choose $\phi = 0$ in the direction defined by the outgoing pion, the 2×4 matrix $A_{\mu\lambda}(\theta, 0)$ is given in Table I.

The differential cross section is the same for either photon helicity because of the parity symmetry. It is

$$\sigma(\theta) = \frac{1}{2} \frac{q}{k} \sum_{i=1}^4 |H_i|^2. \quad (8)$$

To write the recoil nucleon polarization in terms of the helicity amplitudes H_i , we use a coordinate system with z axis along \mathbf{q} and y axis in the direction of $\mathbf{k} \times \mathbf{q}$. Then

TABLE I. Helicity amplitudes $A_{\mu\lambda}(\theta, 0)$.

$\begin{array}{c} \lambda \\ \mu \end{array}$	$\lambda_k = +1$		$\lambda_k = -1$	
	$\frac{3}{2}$	$\frac{1}{2}$	$-\frac{1}{2}$	$-\frac{3}{2}$
$\frac{1}{2}$	H_1	H_2	H_4	$-H_3$
$-\frac{1}{2}$	H_3	H_4	$-H_2$	H_1

for photon helicity $\lambda_k = +1$, Eq. (6) gives

$$\mathbf{P} \cdot (\hat{k} \times \hat{q}) = -\frac{1}{2} \frac{q}{k} \frac{1}{\sigma(\theta)} \text{Tr} A^\dagger \sigma_y A,$$

so that the polarization in the direction $\hat{k} \times \hat{q}$ is

$$P(\theta) = -\frac{q}{k} \frac{1}{\sigma(\theta)} \text{Im}(H_1 H_3^* + H_2 H_4^*). \quad (9)$$

The same result holds for photon helicity $\lambda_k = -1$ because of the parity symmetry.

Next we wish to find the asymmetry for linearly polarized incident photons. The (circularly polarized) helicity states of the photon have polarization vectors

$$\boldsymbol{\epsilon}_\pm = \mp (1/\sqrt{2})(\hat{e}_x \pm i\hat{e}_y), \quad \lambda_k = \pm 1 \quad (10)$$

where \hat{e}_x and \hat{e}_y are unit vectors along the x and y axes of a coordinate system with z axis along \mathbf{k} and y axis in the direction of $\mathbf{k} \times \mathbf{q}$. Thus \mathbf{q} is in the xz plane and has $\phi = 0$. Linearly polarized photons with electric vectors perpendicular or parallel to the production plane have polarization vectors $\boldsymbol{\epsilon}_\perp$ and $\boldsymbol{\epsilon}_\parallel$, respectively, where

$$\begin{aligned} \boldsymbol{\epsilon}_\perp &= \hat{e}_y = (i/\sqrt{2})(\boldsymbol{\epsilon}_+ + \boldsymbol{\epsilon}_-), \\ \boldsymbol{\epsilon}_\parallel &= \hat{e}_x = -(1/\sqrt{2})(\boldsymbol{\epsilon}_+ - \boldsymbol{\epsilon}_-). \end{aligned} \quad (11)$$

Combining the helicity amplitudes of Table I according to these relations, we obtain the amplitudes for linearly polarized photons given in Table II.

From Table II, the cross sections for polarized photons are

$$\begin{aligned} \sigma_\perp(\theta) &= \frac{1}{2} (q/k) (|H_1 + H_4|^2 + |H_2 - H_3|^2), \\ \sigma_\parallel(\theta) &= \frac{1}{2} (q/k) (|H_1 - H_4|^2 + |H_2 + H_3|^2). \end{aligned} \quad (12)$$

TABLE II. Amplitudes for linearly polarized photons.

$\begin{array}{c} -\lambda_1 \\ \mu = -\lambda_2 \end{array}$	$\boldsymbol{\epsilon}_\perp = \frac{i}{\sqrt{2}}(\boldsymbol{\epsilon}_+ + \boldsymbol{\epsilon}_-)$		$\boldsymbol{\epsilon}_\parallel = -\frac{1}{\sqrt{2}}(\boldsymbol{\epsilon}_+ - \boldsymbol{\epsilon}_-)$	
	$\frac{1}{2}$	$-\frac{1}{2}$	$\frac{1}{2}$	$-\frac{1}{2}$
$\frac{1}{2}$	$\frac{i}{\sqrt{2}}(H_1 + H_4)$	$\frac{i}{\sqrt{2}}(H_2 - H_3)$	$\frac{1}{\sqrt{2}}(H_4 - H_1)$	$-\frac{1}{\sqrt{2}}(H_2 + H_3)$
$-\frac{1}{2}$	$\frac{i}{\sqrt{2}}(H_3 - H_2)$	$\frac{i}{\sqrt{2}}(H_1 + H_4)$	$-\frac{1}{\sqrt{2}}(H_2 + H_3)$	$\frac{1}{\sqrt{2}}(H_1 - H_4)$

¹⁹ M. Jacob and G. C. Wick, Ann. Phys. (N. Y.) 7, 404 (1959).

The polarized photon asymmetry is

$$\Sigma = \frac{\sigma_{\perp} - \sigma_{\parallel}}{\sigma_{\perp} + \sigma_{\parallel}}, \quad (13)$$

$$\Sigma(\theta) = \frac{q}{k} \frac{1}{\sigma(\theta)} \operatorname{Re}(H_1 H_4^* - H_2 H_3^*).$$

Note the interesting comparison between relations (9) and (13), expressing the recoil nucleon polarization and the asymmetry for linearly polarized photons, respectively. Another similar relation, for which no experimental data yet exist, is the asymmetry for a polarized target. If σ_+ and σ_- are the differential cross sections for target nucleons polarized "up" and "down" in the direction of $\mathbf{k} \times \mathbf{q}$, then the polarized target asymmetry is

$$T(\theta) = \frac{\sigma_+ - \sigma_-}{\sigma_+ + \sigma_-}, \quad (14)$$

$$T(\theta) = \frac{q}{k} \frac{1}{\sigma(\theta)} \operatorname{Im}(H_1 H_2^* + H_3 H_4^*).$$

4. Partial-Wave Analysis

Next we wish to write the helicity amplitudes in terms of states of definite angular momentum and parity.

The partial-wave expansion¹⁹

$$A_{\mu\lambda}(\theta, \phi) = \sum_j A_{\mu\lambda}^j (2j+1) d_{\lambda\mu}^j(\theta) e^{i(\lambda-\mu)\phi} \quad (15)$$

expresses $A_{\mu\lambda}(\theta, \phi)$ in terms of the functions

$$(2j+1)^{1/2} d_{\lambda\mu}^j(\theta) e^{i(\lambda-\mu)\phi}, \quad (16)$$

which are mutually orthogonal and normalized to 4π when integrated over $d\Omega$.

The orthogonality of these functions makes it easy to express the integrated cross section σ_T in terms of the helicity coefficients $A_{\mu\lambda}^j \equiv H_i^j$. Integrating Eq. (8),

$$\sigma_T = 2\pi \frac{q}{k} \sum_j \sum_{i=1}^4 (2j+1) |H_i^j|^2. \quad (17)$$

The d functions may be expressed in terms of derivatives of Legendre polynomials.¹⁹ Writing $n = j - \frac{1}{2}$,

$$\begin{aligned} (n+1) d_{3/2, 1/2}^j(\theta) &= -[n(n+2)]^{-1/2} \\ &\quad \times \sin\theta \cos\frac{1}{2}\theta (P_{n+1}'' - P_n''), \\ (n+1) d_{1/2, 1/2}^j(\theta) &= \cos\frac{1}{2}\theta (P_{n+1}' - P_n'), \\ (n+1) d_{3/2, -1/2}^j(\theta) &= [n(n+2)]^{-1/2} \\ &\quad \times \sin\theta \sin\frac{1}{2}\theta (P_{n+1}'' + P_n''), \\ (n+1) d_{1/2, -1/2}^j(\theta) &= -\sin\frac{1}{2}\theta (P_{n+1}' + P_n'). \end{aligned} \quad (18)$$

(Note that the first and third functions vanish for $n=0$, so that the corresponding coefficients $A_{\pm 1/2, 3/2}^{1/2}$ are zero

as they must be since a $j = \frac{1}{2}$ state cannot have helicity $\frac{3}{2}$.)

The helicity coefficients $A_{\mu\lambda}^j$ depend only on the energy W . They may be projected from the helicity amplitudes $A_{\mu\lambda}(\theta, \phi)$ by using the orthonormal properties of functions (16) to invert Eq. (15):

$$A_{\mu\lambda}^j = \frac{1}{4\pi} \int d\Omega A_{\mu\lambda}(\theta, \phi) d_{\lambda\mu}^j(\theta) e^{-i(\lambda-\mu)\phi}. \quad (19)$$

This inversion process was first carried out by Ball.²⁰

The coefficients $A_{\mu\lambda}^j$ refer to states of definite j but mixed parity. Final states of definite parity are formed by the sum and difference of final states having opposite helicity, μ and $-\mu$.²¹ Thus the sum and difference, $A_{1/2, \lambda}^j \pm A_{-1/2, \lambda}^j$, of the two final helicity states for given initial helicity do correspond to definite parity and we call these combinations "helicity elements," defined as follows²²:

$$\begin{aligned} A_{n+} &= -(1/\sqrt{2})(A_{1/2, 1/2}^j + A_{-1/2, 1/2}^j), \\ A_{(n+1)-} &= (1/\sqrt{2})(A_{1/2, 1/2}^j - A_{-1/2, 1/2}^j), \\ B_{n+} &= [2/n(n+2)]^{1/2}(A_{1/2, 3/2}^j + A_{-1/2, 3/2}^j), \quad n \geq 1 \\ B_{(n+1)-} &= -[2/n(n+2)]^{1/2}(A_{1/2, 3/2}^j - A_{-1/2, 3/2}^j), \quad n \geq 1 \end{aligned} \quad (20)$$

where $n = j - \frac{1}{2}$ and the subscript notation of the A 's and B 's corresponds to that of CGLN²³; e.g., $B_{l\pm}$ refers to a state with pion orbital angular momentum l and total angular momentum $j = l \pm \frac{1}{2}$.

Using the definitions (20) to express the $A_{\mu\lambda}^j$ in terms of the A 's and B 's, and putting the explicit expressions (18) for the d functions in Eq. (15), we obtain the following expressions for the helicity amplitudes:

$$\begin{aligned} H_1(\theta, \phi) &\equiv A_{1/2, 3/2} = (1/\sqrt{2}) e^{i\phi} \sin\theta \cos\frac{1}{2}\theta \\ &\quad \times \sum_{n=1}^{\infty} (B_{n+} - B_{(n+1)-}) (P_n'' - P_{n+1}''), \\ H_2(\theta, \phi) &\equiv A_{1/2, 1/2} = \sqrt{2} \cos\frac{1}{2}\theta \\ &\quad \times \sum_{n=0}^{\infty} (A_{n+} - A_{(n+1)-}) (P_n' - P_{n+1}'), \\ H_3(\theta, \phi) &\equiv A_{-1/2, 3/2} = (1/\sqrt{2}) e^{2i\phi} \sin\theta \sin\frac{1}{2}\theta \\ &\quad \times \sum_{n=1}^{\infty} (B_{n+} + B_{(n+1)-}) (P_n'' + P_{n+1}''), \\ H_4(\theta, \phi) &\equiv A_{-1/2, 1/2} = \sqrt{2} e^{i\phi} \sin\frac{1}{2}\theta \\ &\quad \times \sum_{n=0}^{\infty} (A_{n+} + A_{(n+1)-}) (P_n' + P_{n+1}'). \end{aligned} \quad (21)$$

²⁰ J. S. Ball, Phys. Rev. **124**, 2014 (1961).

²¹ See Eq. (41) of Ref. 19.

²² The notation and normalization of the A 's and B 's are taken from Jean Hebb, who first introduced them.

²³ G. F. Chew, M. L. Goldberger, F. E. Low, and Y. Nambu, Phys. Rev. **106**, 1345 (1957).

In terms of the A 's and B 's, the integral cross section is

$$\sigma_T = 4\pi \frac{q}{k} \sum_{n=0}^{\infty} [(n+1)(|A_{n+}|^2 + |A_{(n+)-}|^2) + \frac{1}{4}n(n+1)(n+2)(|B_{n+}|^2 + |B_{(n+)-}|^2)]. \quad (22)$$

5. CGLN Amplitudes

CGLN²³ write the amplitude (4) in terms of the following combinations of Pauli-spin matrices:

$$iA = i\boldsymbol{\sigma} \cdot \boldsymbol{\varepsilon} \mathcal{F}_1 + \boldsymbol{\sigma} \cdot \hat{\mathbf{q}} \boldsymbol{\sigma} \cdot (\hat{\mathbf{k}} \times \boldsymbol{\varepsilon}) \mathcal{F}_2 + i\boldsymbol{\sigma} \cdot \hat{\mathbf{k}} \hat{\mathbf{q}} \cdot \boldsymbol{\varepsilon} \mathcal{F}_3 + i\boldsymbol{\sigma} \cdot \hat{\mathbf{q}} \hat{\mathbf{q}} \cdot \boldsymbol{\varepsilon} \mathcal{F}_4, \quad (23)$$

where $\hat{\mathbf{q}}$ and $\hat{\mathbf{k}}$ are unit vectors along \mathbf{q} and \mathbf{k} . Putting $\boldsymbol{\varepsilon} = \boldsymbol{\varepsilon}_+ = -(1/\sqrt{2})(\hat{\varepsilon}_x + i\hat{\varepsilon}_y)$ for photon helicity $+1$, and taking matrix elements between Pauli spinors corresponding to the appropriate final and initial nucleon helicity states, one obtains the helicity amplitudes in terms of the CGLN \mathcal{F} 's:

$$\begin{aligned} H_1(\theta, \phi) &= -(1/\sqrt{2})e^{i\phi} \sin\theta \cos\frac{1}{2}\theta (\mathcal{F}_3 + \mathcal{F}_4), \\ H_2(\theta, \phi) &= \sqrt{2} \cos\frac{1}{2}\theta [(\mathcal{F}_2 - \mathcal{F}_1) + \frac{1}{2}(1 - \cos\theta)(\mathcal{F}_3 - \mathcal{F}_4)], \\ H_3(\theta, \phi) &= (1/\sqrt{2})e^{2i\phi} \sin\theta \sin\frac{1}{2}\theta (\mathcal{F}_3 - \mathcal{F}_4), \\ H_4(\theta, \phi) &= \sqrt{2}e^{i\phi} \sin\frac{1}{2}\theta [(\mathcal{F}_1 + \mathcal{F}_2) + \frac{1}{2}(1 + \cos\theta)(\mathcal{F}_3 + \mathcal{F}_4)]. \end{aligned} \quad (24)$$

CGLN give a well-known expansion of the \mathcal{F} 's in terms of multipole coefficients $M_{l\pm}$ and $E_{l\pm}$. By using this expansion in (24) and comparing with (21), one can find the following relations between the CGLN multipole coefficients and the helicity elements:

$$E_{0+} = A_{0+}, \quad M_{1-} = A_{1-},$$

and for $l \geq 1$,

$$\begin{aligned} E_{l+} &= (l+1)^{-1}(A_{l+} + \frac{1}{2}lB_{l+}), \\ M_{l+} &= (l+1)^{-1}[A_{l+} - \frac{1}{2}(l+2)B_{l+}], \\ E_{(l+1)-} &= -(l+1)^{-1}[A_{(l+1)-} - \frac{1}{2}(l+2)B_{(l+1)-}], \\ M_{(l+1)-} &= (l+1)^{-1}(A_{(l+1)-} + \frac{1}{2}lB_{(l+1)-}). \end{aligned} \quad (25)$$

6. Born Approximation

The Born approximation, obtained by evaluating the Feynman diagrams of Fig. 1, is conveniently expressed in terms of the CGLN amplitudes \mathcal{F}_i . In the formulas below, the appropriate couplings are to be used for each specific reaction. The couplings G_π for the pion-nucleon vertex are

$$G_{\pi^+} = -G_{\pi^-} = -\sqrt{2}G_{\pi^0 p} = \sqrt{2}G_{\pi^0 n} = \sqrt{2}G, \quad (26)$$

where $G^2/4\pi = 14.7$. ϵ_π , ϵ_1 , and ϵ_2 are the charges in units e of the pion, the initial nucleon, and the final nucleon, respectively. (For example, $\epsilon_\pi = 0$ for π^0 production, and $\epsilon_\pi = -1$ for π^- ; ϵ_1 or $\epsilon_2 = 0$ for a neutron.) μ_1 and μ_2 are the anomalous magnetic moments of the initial and final nucleons, with values 1.793 and -1.913

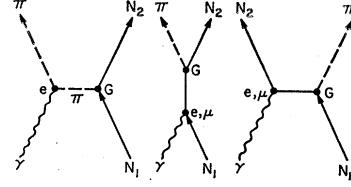


FIG. 1. Feynman diagrams for the Born approximation.

for proton and neutron, respectively. Finally, some square-root signs are avoided in the formulas by letting $Z_1 = (E_1 + M_1)^{1/2}$ and $Z_2 = (E_2 + M_2)^{1/2}$.

The Born approximation for electric coupling e is

$$\begin{aligned} \mathcal{F}_1 &= -\frac{eG_\pi}{4\pi} \frac{Z_1 Z_2}{W + M_1} \left(\frac{\epsilon_1}{2W} + \frac{k\epsilon_2}{u - M_2^2} \right), \\ \mathcal{F}_2 &= \frac{eG_\pi}{4\pi} \frac{qZ_1}{Z_2(W + M_1)} \left(\frac{\epsilon_1}{2W} + \frac{k\epsilon_2}{u - M_2^2} \right), \\ \mathcal{F}_3 &= \frac{eG_\pi}{4\pi} \frac{qkZ_2}{WZ_1} \left(\frac{\epsilon_\pi}{t - m_\pi^2} - \frac{\epsilon_2}{u - M_2^2} \right), \\ \mathcal{F}_4 &= -\frac{eG_\pi}{4\pi} \frac{q^2 Z_1}{WZ_2} \left(\frac{\epsilon_\pi}{t - m_\pi^2} - \frac{\epsilon_2}{u - M_2^2} \right). \end{aligned} \quad (27)$$

The Born approximation for the anomalous magnetic moment terms is

$$\begin{aligned} \mathcal{F}_1 &= \frac{eG_\pi}{4\pi} \frac{kZ_2}{4WZ_1} \left(\frac{\mu_1}{M_1} - \frac{\mu_2 Z_1^2}{kM_2} - \frac{2\mu_2(W + M_1)}{u - M_2^2} \right), \\ \mathcal{F}_2 &= \frac{eG_\pi}{4\pi} \frac{qk}{4WZ_1 Z_2} \left(\frac{\mu_1 Z_1^2}{M_1 k} - \frac{\mu_2}{M_2} + \frac{2\mu_2(W + M_1)}{u - M_2^2} \right), \\ \mathcal{F}_3 &= -\frac{eG_\pi}{4\pi} \frac{\mu_2 qk}{2WM_2 Z_1} \frac{Z_2 W + M_1}{u - M_2^2}, \\ \mathcal{F}_4 &= -\frac{eG_\pi}{4\pi} \frac{\mu_2 qk}{2WM_2 Z_1 Z_2} \frac{q}{u - M_2^2} \frac{W + M_1}{u - M_2^2}. \end{aligned} \quad (28)$$

7. Isospin Decomposition

The photon interaction has an isovector part and an isoscalar part. The vector part gives final states of isospin $\frac{3}{2}$ and $\frac{1}{2}$, with amplitudes A^{V3} and A^{V1} , respectively. The scalar part gives final states of isospin $\frac{1}{2}$ with amplitude A^S . Amplitudes for the four physical photopion reactions may be written in terms of these in a form first given by Watson²⁴:

$$\begin{aligned} \pi^+ : A^+ &= (\sqrt{\frac{1}{3}})A^{V3} - (\sqrt{\frac{2}{3}})(A^{V1} - A^S), \\ \pi^0 : A^0 &= (\sqrt{\frac{2}{3}})A^{V3} + (\sqrt{\frac{1}{3}})(A^{V1} - A^S), \\ \pi^- : A^- &= (\sqrt{\frac{1}{3}})A^{V3} - (\sqrt{\frac{2}{3}})(A^{V1} + A^S), \\ n\pi^0 : A^{n0} &= (\sqrt{\frac{2}{3}})A^{V3} + (\sqrt{\frac{1}{3}})(A^{V1} + A^S). \end{aligned} \quad (29)$$

²⁴ K. M. Watson, Phys. Rev. **85**, 852 (1952).

8. Resonances

The following Breit-Wigner form is used for a resonant amplitude:

$$A(W) = A(W_0) \left(\frac{k_0 q_0}{kq} \right)^{1/2} \frac{W_0 \Gamma^{1/2} \Gamma_\gamma^{1/2}}{s_0 - s - iW_0 \Gamma}, \quad (30)$$

where

$$\Gamma = \Gamma_0 \left(\frac{q}{q_0} \right)^{2l+1} \left(\frac{q_0^2 + X^2}{q^2 + X^2} \right)^l, \quad (31)$$

$$\Gamma_\gamma = \Gamma_0 \left(\frac{k}{k_0} \right)^{2j_\gamma} \left(\frac{k_0^2 + X^2}{k^2 + X^2} \right)^{j_\gamma},$$

where W_0 is the "mass" of the resonance, and $k_0, q_0,$ and s_0 are the values of $k, q,$ and s at the resonance energy $W = W_0$. A resonance is thus described by the parameters $W_0, \Gamma_0, A(W_0), l, j_\gamma,$ and X .

IV. PROCEDURE

Among the individual reactions

$$\begin{aligned} \pi^+ : \gamma + p &\rightarrow \pi^+ + n, \\ \pi^0 : \gamma + p &\rightarrow \pi^0 + p, \\ \pi^- : \gamma + n &\rightarrow \pi^- + p, \\ n\pi^0 : \gamma + n &\rightarrow \pi^0 + n, \end{aligned} \quad (32)$$

the first two have been investigated most thoroughly, both experimentally and in the present analysis. Data on the π^- reaction are still rather limited and the π^- fits must be regarded as tentative. No consideration has yet been given to the fourth reaction ($n\pi^0$). The param-

eters used in fitting the separate reactions have been treated as independent except that the resonances are ascribed to specific isospin states so that their relative contribution to π^+ and π^0 production is given by the appropriate Clebsch-Gordan coefficients as in Eqs. (29).

Variation of the parameters in order to obtain a fit to the data was carried out not by a computer search but in the following subjective manner: Using a set of trial values of the parameters, the quantities $\sigma(\theta), P(\theta),$ and $\Sigma(\theta)$ were calculated for comparison with the data, and the helicity amplitudes $H_i(\theta)$ were also printed out. By considering the effect of the parameters $A_{l\pm}$ and $B_{l\pm}$ on the helicity amplitudes as shown graphically in Fig. 2 and the resulting effect on $\sigma(\theta), P(\theta),$ and $\Sigma(\theta),$ as given by Eqs. (8), (9), and (13), it was generally possible to find an improved set of values for the parameters. The values of the parameters obtained in this way were then plotted as functions of energy and changes were made in an attempt to smooth out the energy-dependent curves. This effort was only partially successful, as may be seen from the results quoted in Sec. V.

Other prejudices applied when varying the parameters were (a) to keep the added contributions $\Delta A_{l\pm}$ and $\Delta B_{l\pm}$ as small as possible, especially for the $j = \frac{5}{2}$ terms, and (b) to avoid introducing imaginary parts in these added terms, except where variation of the real parts was inadequate to fit the data. An exception is the imaginary parts of A_{0+} for π^+ and $\pi^0,$ which have been chosen in the low-energy region to make the A_{0+} phases approximately equal to the relevant πN scattering phase shifts.

Evidence for a resonance may show up in two ways. If a large imaginary part for some amplitude seems needed in a given energy region, a natural way to supply it is to make this amplitude resonant. The other way in which a resonance may manifest itself is by producing a rapid variation with energy in the real part of the corresponding amplitude. If both types of evidence exist, the relative signs must be self-consistent, providing a check. Typical behaviors of the real and imaginary parts of a resonant amplitude are shown in Fig. 3.

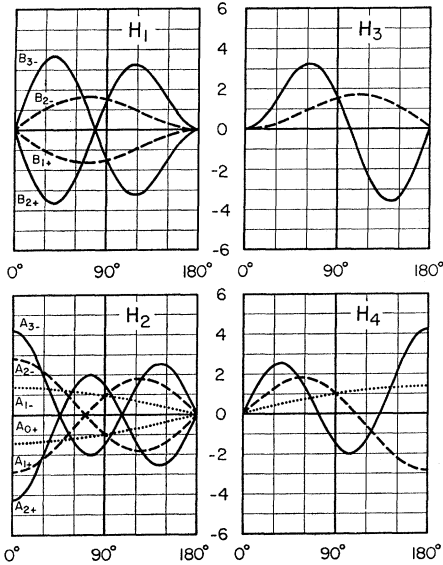


FIG. 2. Contributions to the four helicity amplitudes $H_n(\theta)$ of individual helicity elements with $j \leq \frac{5}{2}$. A curve marked B_{l+} , for example, corresponds to a value unity for the element B_{l+} , and all other parameters equal zero. These curves are simply the functions $d_{\lambda,\mu}^j(\theta)$, suitably normalized.

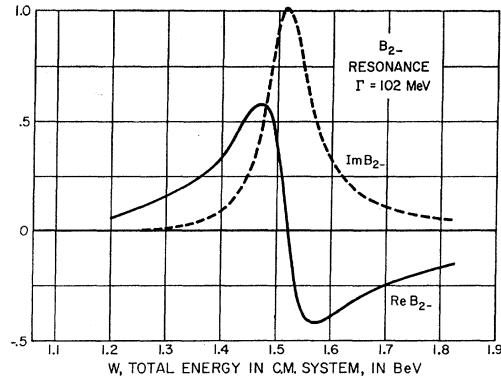


FIG. 3. Typical behavior of the real and imaginary parts of a resonant amplitude. The resonance parameters are those of the $B_{2-}(1519)$ resonance of Table III, except the amplitude is unity.

TABLE III. Resonance parameters used in the Breit-Wigner formula of Sec. III 8. $A^+(W_0)$, $A^0(W_0)$, and $A^-(W_0)$ are the amplitudes at resonance for the physical reactions $\gamma p \rightarrow \pi^+ n$, $\gamma p \rightarrow \pi^0 p$, and $\gamma n \rightarrow \pi^- p$, respectively.

Resonant helicity element	Iso-spin T	Energy W_0 (BeV)	Width Γ_0 (BeV)	l	j_γ	X (BeV)	$A^+(W_0)$ ($\mu\text{b}^{1/2}$)	$A^0(W_0)$ ($\mu\text{b}^{1/2}$)	$A^-(W_0)$ ($\mu\text{b}^{1/2}$)
A_{1+}	$\frac{3}{2}$	1.236	0.120	1	1	0.160	1.000	1.414	1.000
B_{1+}	$\frac{3}{2}$	1.236	0.120	1	1	0.160	-2.430	-3.430	-2.430
A_{2-}	$\frac{1}{2}$	1.519	0.102	2	1	0.350	-0.200	0.140	0
B_{2-}	$\frac{1}{2}$	1.519	0.102	2	1	0.350	-1.320	0.940	-1.150
B_{3-}	$\frac{1}{2}$	1.672	0.104	3	2	0.350	-0.600	0.425	-0.500
A_{0+}	$\frac{1}{2}$	1.561	0.180	0	1	0.350	-0.650	0.460	-0.800
A_{1-}	$\frac{1}{2}$	1.471	0.200	1	1	0.350	-0.250	0.177	0*
B_{2+}	$\frac{1}{2}$	1.652	0.134	2	2	0.350	0.141	-0.100	0.141

* An A_{1-} resonance in π^- photoproduction with amplitude -0.250 could be used to supply the imaginary A_{1-} contribution of Table VI. However, the behavior of the real part of ΔA_{1-} indicates, if anything, a resonance with the opposite sign. Thus neither the presence nor the absence of the A_{1-} (1471) resonance seems to be established in π^- production.

V. RESULTS

In Table III are listed values of the parameters for the resonances used in the fit. The resonant amplitudes are obtained from these parameters according to the formulas of Sec. III 8. The energies and widths of the resonances were taken from a table due to Lovelace.²⁵

In Tables IV-VI are listed values of the extra contributions in the low partial waves added to the resonances and electric Born terms [contribution (3) of Sec. II]. As mentioned when describing the procedure, an attempt was made to find a fit in which the energy dependence of these adjustable contributions would be smooth and, if possible, free from large variations. Although the variations with energy shown in Tables IV-VI are greater than I would like, this attempt was probably as successful as one might expect in view of the simple model and fitting procedure. In fact, most of the rapid variations occur in amplitudes which are resonant, in the energy region of the resonance. This behavior should be allowed in order to correct for the inadequacy of the simple Breit-Wigner resonance formula and because the choice of resonance energies and widths may not be optimal. Finally, some rapid variations in A_{0+} for π^+ and π^0 near $W=1.5$ BeV were included purposely to account for the behavior of the π^+ cross sections at 0° and 180° in this energy region. This point will be discussed in Sec. VI 10.

The added contributions $\Delta A_{l\pm}$ and $\Delta B_{l\pm}$ are given in Tables IV-VI for the physical charge states rather than for isospin states, because this is the form in which they have entered the fitting procedure, and conversion to isospin states could be misleading. For example, suppose the π^0 data require an imaginary part of an amplitude A_{1-} in some energy region, whereas the π^+ data are quite insensitive to $\text{Im}A_{1-}$, which is therefore left equal to zero. Conversion to isospin- $\frac{1}{2}$ and $-\frac{3}{2}$ amplitudes would make each of them appear significant, although neither would have been well determined.

The total helicity elements projected from the complete photoproduction amplitudes are given in Tables VII-IX for partial waves with $j \leq \frac{5}{2}$. Higher partial waves have the Born-approximation values.

Some of the fits resulting from the parameters of Tables III-VI are shown together with experimental data in Figs. 4-8. Data which were taken into account when making the fits are to be found in the following references, grouped according to the type of measurement:

(1) π^+ differential cross sections: Refs. 26-44.

²⁶ R. L. Walker, J. G. Teasdale, V. Z. Peterson, and J. I. Vette, *Phys. Rev.* **99**, 210 (1955).

²⁷ S. D. Ecklund and R. L. Walker, *Phys. Rev.* **159**, 1195 (1967).

²⁸ M. Beneventano, G. Bernardini, D. Carlson-Lee, G. Stoppini, and L. Tau [Nuovo Cimento **4**, 323 (1956)] include data from the following: G. Bernardini and E. L. Goldwasser, *Phys. Rev.* **94**, 729 (1954); **95**, 857 (1954); also, T. L. Jenkins, D. Luckey, T. R. Palfrey, and R. R. Wilson, *ibid.* **95**, 179 (1954).

²⁹ M. Beneventano, R. Finzi, L. Mezzetti, L. Paoluzi, and S. Tazzari, *Nuovo Cimento* **28**, 1464 (1963).

³⁰ A. V. Tolstrup, J. C. Keck, and R. M. Worlock, *Phys. Rev.* **99**, 220 (1955).

³¹ H. A. Thiessen, *Phys. Rev.* **155**, 1488 (1967).

³² D. Freytag, W. J. Schuille, and R. J. Wedemeyer, *Z. Physik* **186**, 1 (1965).

³³ C. Freitag, D. Freytag, K. Lubelsmeyer, and W. Paul, *Z. Physik* **175**, 1 (1963).

³⁴ M. I. Adamovich, E. G. Gorzhenskaya, V. G. Larionova, N. M. Panova, S. P. Kharlamov, and F. R. Yagudina, in *Proceedings of the International Conference on High-Energy Physics, Geneva, 1962*, edited by J. Prentki (CERN, Geneva, 1962), p. 207; also, A. M. Baldin, in *Proceedings of the Tenth Annual International Conference on High-Energy Physics, Rochester, 1960*, edited by E. C. G. Sudarshan (Wiley-Interscience, Inc., New York, 1961), pp. 26, 330.

³⁵ J. C. Bizot, J. Perez y Jorba, and D. Treille, *Phys. Letters* **7**, 489 (1967).

³⁶ K. Althoff, H. Fischer, and W. Paul, *Z. Physik* **175**, 19 (1963).

³⁷ L. Hand and C. Schaerf, *Phys. Rev. Letters* **6**, 229 (1961).

³⁸ C. Schaerf, *Nuovo Cimento* **44**, 504 (1966).

³⁹ Alan J. Lazarus, W. K. H. Panofsky, and F. R. Tangherlini, *Phys. Rev.* **113**, 1330 (1959).

⁴⁰ D. W. G. S. Leith, R. Little, and E. M. Lawson, *Phys. Letters* **8**, 355 (1964).

⁴¹ R. A. Alvarez, *Phys. Rev.* **142**, 957 (1966).

⁴² Edward A. Knapp, Robert W. Kenney, and Victor Perez-Mendez, *Phys. Rev.* **114**, 605 (1959).

⁴³ R. J. Walker, T. R. Palfrey, Jr., R. O. Haxby, and B. M. K. Nefkens, *Phys. Rev.* **132**, 2656 (1963).

⁴⁴ M. Heineberg, W. M. McClelland, F. Turkot, W. M. Woodward, R. R. Wilson, and D. M. Zipoy, *Phys. Rev.* **110**, 1211 (1958).

²⁵ See P. G. Murphy, in *Proceedings of the Thirteenth International Conference on High-Energy Physics, Berkeley, 1966* (University of California Press, Berkeley, 1967), p. 176.

- (2) π^0 differential cross sections: Refs. 45-65.
 - (3) π^- differential cross sections: Refs. 66-68.
 - (4) Recoil proton polarization for π^0 : Refs. 69-76.
 - (5) Recoil proton polarization for π^- : Ref. 77.
 - (6) Recoil neutron polarization for π^+ : Ref. 78.
 - (7) π^+ asymmetry from polarized photons: Refs. 79-83.
 - (8) π^0 asymmetry from polarized photons: Refs. 84-86.
- (Not all of the data considered are shown in Figs. 4-8.)

⁴⁵ D. C. Oakley and R. L. Walker, Phys. Rev. **97**, 1283 (1955).
⁴⁶ R. Diebold, Phys. Rev. **130**, 2089 (1963).
⁴⁷ W. S. McDonald, V. Z. Peterson, and D. R. Corson, Phys. Rev. **107**, 577 (1957).
⁴⁸ J. I. Vette, Phys. Rev. **111**, 622 (1958).
⁴⁹ G. Fischer, H. Fischer, H. J. Kampgen, G. Knop, P. Schulz, and H. Wessels, University of Bonn Report, 1966 (unpublished).
⁵⁰ C. R. Clinesmith, G. L. Hatch, and A. V. Tollestrup, in *Proceedings of the International Symposium on Electron and Photon Interactions at High Energies* (Deutsche Physikalische Gesellschaft, Hamburg, Germany, 1966), Vol. II, p. 245; also, C. R. Clinesmith and G. L. Hatch, Ph.D. theses, California Institute of Technology, 1967 (unpublished).
⁵¹ L. J. Koester, Jr., and F. E. Mills, Phys. Rev. **105**, 1900 (1957).
⁵² R. M. Talman, Ph.D. thesis, California Institute of Technology, 1963 (unpublished); see also R. M. Talman, C. R. Clinesmith, R. Gomez, and A. V. Tollestrup, Phys. Rev. Letters **9**, 177 (1962).
⁵³ R. G. Vasil'kov, B. B. Govorkov, and V. I. Gol'danskii, Zh. Eksperim. i Teor. Fiz. **37**, 11 (1959) [English transl.: Soviet Phys.—JETP **10**, 7 (1960)].
⁵⁴ C. Ward, B. Kenton, and C. York, Phys. Rev. **159**, 1176 (1967).
⁵⁵ C. Bacci, G. Penso, G. Salvini, C. Mencuccini, A. Reale, V. Silvestrini, M. Spinetti, and B. Stella, Phys. Rev. **159**, 1124 (1967).
⁵⁶ Karl Berkelman and James A. Waggoner, Phys. Rev. **117**, 1364 (1960).
⁵⁷ R. M. Worlock, Phys. Rev. **117**, 537 (1960).
⁵⁸ V. L. Highland and J. W. DeWire, Phys. Rev. **132**, 1293 (1963).
⁵⁹ H. De Staebler, Jr., E. F. Erickson, A. C. Hearn, and C. Schaerf, Phys. Rev. **140**, B336 (1965).
⁶⁰ D. B. Miller and E. H. Bellamy, Proc. Phys. Soc. (London) **81**, 343 (1963).
⁶¹ J. W. DeWire, H. E. Jackson, and Raphael Littauer, Phys. Rev. **110**, 1208 (1958).
⁶² P. C. Stein and K. C. Rogers, Phys. Rev. **110**, 1209 (1958).
⁶³ G. Bellettini, C. Bemporad, P. J. Biggs, and P. L. Braccini, Nuovo Cimento **44**, 239 (1966); G. Bellettini, C. Bemporad, P. L. Braccini, L. Foa, and E. H. Bellamy, *ibid.* **29**, 1195 (1963).
⁶⁴ H. E. Jackson, J. W. DeWire, and R. M. Littauer, Phys. Rev. **119**, 1381 (1960).
⁶⁵ B. B. Govorkov, S. P. Denisov, A. I. Lebedev, E. V. Minarik, and S. P. Kharlamov, Zh. Eksperim. i Teor. Fiz. **47**, 1199 (1964) [English transl.: Soviet Phys.—JETP **20**, 809 (1965)]; B. B. Govorkov, S. P. Denisov, and E. V. Minarik, in *Proceedings of the International Conference on High-Energy Physics, Geneva, 1962*, edited by J. Prentki (CERN, Geneva, 1962), p. 213.
⁶⁶ Gerry Neugebauer, Walter Wales, and R. L. Walker, Phys. Rev. **119**, 1726 (1960).
⁶⁷ M. Beneventano, G. Bernardini, G. Stoppini, and L. Tau, Nuovo Cimento **10**, 1109 (1958).
⁶⁸ Matthew Sands, J. G. Teasdale, and Robert L. Walker, Phys. Rev. **95**, 592 (1954).
⁶⁹ D. E. Lundquist, R. L. Anderson, J. V. Allaby, and D. M. Ritson, Phys. Rev. **168**, 1527 (1968).
⁷⁰ K. H. Althoff, K. Kramp, H. Matthäy, and H. Piel, Z. Physik **194**, 135 (1966); **194**, 144 (1966); K. H. Althoff, D. Finken, N. Minatti, H. Piel, D. Trines, and M. Unger, in *Proceedings of the 1967 International Symposium on Electron and Photon Inter-*

TABLE VI. Contributions to the helicity elements for the reaction $\gamma n \rightarrow \pi^- p$, added to the resonance and Born terms. (See caption of Table IV.)

k_{lab} (BeV)	0.180	0.200	0.280	0.250	0.300	0.330	0.370	0.400	0.460	0.505	0.600	0.700	0.790	0.875	0.965
ΔA_{0+}	0.26	0.30	0.49	0.43	0.53	0.58	0.63	0.65	0.62	0.60	0.60	0.70	0.87	0.92	0.88
ΔA_{1-}	0.35	0.40	0.61	0.53	0.65	0.72	0.83	0.90	1.03	1.13	1.35	1.40	1.33	1.28	1.26
									(-0.04)	(-0.09)	(-0.19)	(-0.25)	(-0.22)	(-0.15)	(-0.07)
ΔA_{1+}	0.06	0.08	0.12	0.11	0.12	0.10	0.07	0.05	-0.02	-0.05	-0.11	-0.15	-0.10	-0.05	0
											(-0.05)	(-0.10)	(-0.10)	(-0.05)	
ΔB_{1+}	0	0.05	0.25	0.18	0.30	0.36	0.42	0.45	0.50	0.53	0.58	0.61	0.63	0.68	0.72
									(0.02)	(0.05)	(0.14)	(0.20)	(0.18)	(0.13)	(0.07)
ΔA_{2-}	0	-0.03	-0.14	-0.11	-0.15	-0.15	-0.13	-0.11	-0.08	-0.05	0	0.05	0.01	0	0
ΔB_{2-}	0.30	0.30	0.30	0.30	0.30	0.30	0.31	0.32	0.35	0.38	0.50	0.75	0.85	0.90	0.90
													(0.17)	(0.15)	(0.05)
ΔB_{2+}	0	0.01	0.04	0.03	0.05	0.06	0.08	0.08	0.09	0.10	0.12	0.15	0.16	0.17	0.18
													(0.03)	(0.04)	(0.05)

TABLE VII. Total helicity elements projected from the complete amplitudes for $\gamma p \rightarrow \pi^+ n$,

k_{lab} (BeV)	0.200	0.250	0.300	0.350	0.400	0.450	0.500	0.550	0.603	0.647
W (BeV)	1.121	1.162	1.201	1.240	1.277	1.313	1.349	1.383	1.418	1.447
A_{0+}	-3.26 (-0.01)	-2.75 (-0.01)	-2.35 (-0.02)	-2.00 (-0.03)	-1.84 (-0.04)	-1.78 (-0.06)	-1.75 (-0.09)	-1.69 (-0.12)	-1.65 (-0.18)	-1.61 (-0.25)
A_{1-}	-0.26	-0.42	-0.50 (-0.01)	-0.53 (-0.01)	-0.55 (-0.02)	-0.56 (-0.04)	-0.57 (-0.08)	-0.55 (-0.14)	-0.50 (-0.21)	-0.41 (-0.25)
A_{1+}	0.11 (0.04)	0.36 (0.26)	0.36 (0.81)	-0.26 (0.97)	-0.49 (0.62)	-0.51 (0.38)	-0.52 (0.26)	-0.51 (0.18)	-0.50 (0.14)	-0.46 (0.11)
B_{1+}	-1.68 (-0.11)	-2.42 (-0.63)	-2.35 (-1.98)	-0.72 (-2.37)	-0.02 (-1.50)	-0.02 (-0.92)	-0.10 (-0.62)	-0.18 (-0.45)	-0.26 (-0.31)	-0.29 (-0.24)
A_{2-}	0.10	0.13	0.13	0.13	0.11	0.10	0.09 (-0.01)	0.08 (-0.01)	0.10 (-0.03)	0.09 (-0.06)
B_{2-}	-0.24	-0.50	-0.65	-0.76	-0.85	-0.92 (0.04)	-1.01 (0.07)	-1.11 (0.07)	-1.22 (-0.03)	-1.35 (-0.22)
A_{2+}	-0.09	-0.12	-0.13	-0.13	-0.13	-0.14	-0.16	-0.17	-0.17	-0.17
B_{2+}	-0.10	-0.16	-0.18	-0.20	-0.20	-0.20	-0.20	-0.20	-0.19	-0.19 (0.01)
A_{3-}	0.03	0.05	0.07	0.07	0.07	0.07	0.07	0.07	0.07	0.06
B_{3-}	-0.05	-0.11	-0.15	-0.18	-0.20	-0.22	-0.24	-0.25	-0.25 (-0.01)	-0.27 (-0.01)

It is clear from Figs. 4-8 that some of the data are not reproduced very well by the present parametrization. In some cases, the discrepancy is not significant in the sense that it could be easily removed by making small changes in the parameters. For example, in the region of the $N^*(1236)$ resonance, the new π^0 data from Bonn⁴⁹ do not agree in normalization with older data. Either can be fitted well by varying the dominant A_{1+} and B_{1+} amplitudes by small amounts.

On the other hand, a number of deviations from the data are difficult to improve. Some of these are:

- (1) The π^+ differential cross section at $k=0.813$ BeV at backward angles.
- (2) The π^+ differential cross sections at the highest energies $k \approx 1.2$ BeV.
- (3) The π^0 cross sections and polarizations in the region 0.700-0.800 BeV.
- (4) The π^0 polarization data in the region 0.500-0.600 BeV.
- (5) The polarized photon asymmetry for π^+ at 90° c.m. in the region 0.500-0.800 MeV.
- (6) The π^0 differential cross sections in the higher-energy region are probably not correctly represented, but the present data are inadequate. New data should be available soon to improve this situation.

VI. OBSERVATIONS AND DISCUSSION

A number of observations on the way in which certain features of the data determine some of the fitting parameters will be made in this section.

1. π^0 Production near First Resonance

In the energy region near 300 MeV, π^0 photoproduction is dominated by the $N^*(1236)$ resonance. As a result, the helicity amplitudes are predominantly imaginary so that the differential cross section is insensitive to small changes in the real parts of other amplitudes, but is quite sensitive to small changes in the imaginary parts. The helicity amplitudes $H_n(\theta)$ at $k=350$ MeV are shown in Fig. 9. The differential cross section near 90° comes mainly from the imaginary part of B_{1+} , whereas the differential cross sections at 0° and 180° come mainly from the imaginary parts of H_2 and H_4 , respectively.

actions at High Energies (Stanford Linear Accelerator Center, Stanford, Calif., 1967), p. 593.

⁷¹ R. Querzoli, G. Salvini, and A. Silverman, *Nuovo Cimento* **19**, 53 (1961).

⁷² C. Mencuccini, R. Querzoli, and G. Salvini, *Phys. Rev.* **126**, 1181 (1962).

⁷³ L. Bertanza, P. Franzini, I. Mannelli, and G. V. Silvestrini, *Nuovo Cimento* **19**, 953 (1961).

⁷⁴ J. O. Maloy, G. A. Salandini, A. Manfredini, V. Z. Peterson, J. I. Friedman, and H. Kendall, *Phys. Rev.* **122**, 1338 (1961).

⁷⁵ P. C. Stein, *Phys. Rev. Letters* **2**, 473 (1959).

⁷⁶ E. Bloom, C. Heusch, C. Prescott, and L. Rochester, *Phys. Rev. Letters* **19**, 671 (1967).

⁷⁷ J. R. Kenemuth and P. C. Stein, *Phys. Rev.* **129**, 2259 (1963).

⁷⁸ K. H. Althoff, H. Piel, W. Wallraff, and G. Wessels, *Phys. Letters* **26B**, 640 (1968).

⁷⁹ F. F. Liu and S. Vitale, *Phys. Rev.* **144**, 1093 (1966).

⁸⁰ R. C. Smith and R. F. Mozley, *Phys. Rev.* **130**, 2429 (1963).

⁸¹ P. Gorenstein, M. Grilli, P. Spillantini, M. Nigro, E. Schiavuta, F. Soso, and V. Valente, *Phys. Letters* **19**, 157 (1965).

⁸² P. Gorenstein, M. Grilli, F. Soso, P. Spillantini, M. Nigro, E. Schiavuta, and V. Valente, *Phys. Letters* **23**, 394 (1966).

⁸³ R. E. Taylor and R. F. Mozley, *Phys. Rev.* **117**, 835 (1960).

⁸⁴ Darrell J. Drickey and Robert F. Mozley, *Phys. Rev.* **136**, B543 (1964); *Phys. Rev. Letters* **8**, 291 (1962).

⁸⁵ R. Zdarko and R. F. Mozley (private communication).

⁸⁶ G. Barbiellini, G. Bologna, J. DeWire, G. Diambri, G. P. Murtas, and G. Sette, in *Proceedings of the Twelfth International Conference on High-Energy Physics, Dubna, 1964* (Atomizdat, Moscow, 1966), Vol. I, p. 838.

in units of $\mu b^{1/2}$. Imaginary parts, where nonzero, are given in parentheses.

0.698	0.752	0.813	0.857	0.902	0.951	1.002	1.056	1.102	1.162	1.204
1.480	1.514	1.551	1.578	1.604	1.632	1.662	1.692	1.717	1.750	1.772
-1.66 (-0.38)	-1.26 (-0.54)	-0.93 (-0.65)	-0.83 (-0.61)	-0.79 (-0.50)	-0.70 (-0.38)	-0.63 (-0.28)	-0.53 (-0.20)	-0.46 (-0.16)	-0.39 (-0.12)	-0.35 (-0.10)
-0.30 (-0.24)	-0.22 (-0.20)	-0.19 (-0.14)	-0.18 (-0.12)	-0.19 (-0.09)	-0.22 (-0.08)	-0.25 (-0.06)	-0.27 (-0.05)	-0.26 (-0.05)	-0.27 (-0.04)	-0.26 (-0.04)
-0.41 (0.09)	-0.35 (0.07)	-0.29 (0.06)	-0.25 (0.05)	-0.21 (0.05)	-0.20 (0.04)	-0.19 (0.04)	-0.17 (0.03)	-0.16 (0.03)	-0.15 (0.03)	-0.14 (0.03)
-0.33 (-0.19)	-0.35 (-0.14)	-0.38 (-0.11)	-0.38 (-0.08)	-0.39 (-0.07)	-0.42 (-0.05)	-0.46 (-0.04)	-0.49 (0)	-0.50 (0.03)	-0.51 (0.04)	-0.51 (0.04)
0.09 (-0.13)	0.20 (-0.20)	0.30 (-0.14)	0.31 (-0.09)	0.30 (-0.06)	0.29 (-0.04)	0.27 (-0.03)	0.22 (-0.02)	0.18 (-0.02)	0.15 (-0.02)	0.12 (-0.01)
-1.38 (-0.70)	-0.74 (-1.31)	-0.06 (-0.98)	0.01 (-0.69)	-0.03 (-0.50)	-0.08 (-0.38)	-0.12 (-0.31)	-0.16 (-0.26)	-0.18 (-0.23)	-0.20 (-0.21)	-0.22 (-0.19)
-0.16 (0.01)	-0.16 (0.02)	-0.15 (0.04)	-0.15 (0.06)	-0.15 (0.09)	-0.13 (0.13)	-0.20 (0.15)	-0.11 (0.13)	-0.09 (0.08)	-0.09 (0.05)	-0.09 (0.04)
0.06 (-0.30)	0.06 (-0.33)	0.05 (-0.38)	0.05 (-0.44)	0.05 (-0.50)	0.03 (-0.50)	0.02 (-0.34)	0.01 (-0.06)	0.01 (-0.03)	0.01 (0)	0.01 (0.04)
-0.02 (-0.02)	-0.03 (-0.03)	-0.06 (-0.06)	-0.10 (-0.10)	-0.19 (-0.19)	-0.35 (-0.35)	-0.55 (-0.55)	-0.54 (-0.54)	-0.44 (-0.44)	-0.31 (-0.31)	-0.25 (-0.25)

By comparing the average cross section at 0° and 180° with the cross section near 90° , we could determine the relative amounts of A_{1+} and B_{1+} contributing to the resonance. This is equivalent to the old question of how much electric quadrupole term E_{1+} contributes to this resonance, which is predominantly the magnetic dipole term M_{1+} . On the other hand, the difference in the cross sections at 0° and 180° is sensitive to the imaginary part of odd-parity terms, the most likely candidate being the S -wave A_{0+} . The imaginary part of A_{0+} in this energy region is of theoretical interest because it makes an important contribution to the sum rule of Fubini, Furlan, and Rossetti.⁸⁷ However, in order to make use of these simple observations, accurate and self-consistent data are needed near 0° , 180° , and 90° over the energy range 300–360 MeV.

2. Small-Angle π^+ Production above First Resonance

A uniform feature of π^+ photoproduction at all energies above about 400 MeV is a very sharp forward peak in the angular distribution. It is interesting to notice how the helicity amplitudes $H_n(\theta)$ which come from the one-pion-exchange term produce this effect. A related observation is that the qualitative features of π^+ photoproduction at energies above the third resonance, near 1200 MeV, can be reproduced by a crude absorption model based on the electric Born-approximation cross section. In Fig. 10 are plotted the helicity amplitudes $H_n(\theta)$ at 1200 MeV which arise from the electric Born approximation alone and from the electric Born approximation with all contributions in the angular momentum states $j=\frac{1}{2}$ and $\frac{3}{2}$ removed. The resulting

⁸⁷ See Ref. 3.

angular distributions are shown, together with the experimental data, in Fig. 11. The sharp forward peak in $\sigma(\theta)$ is due entirely to the corresponding peak in $H_2(\theta)$, and this comes from the coherent combination of many high partial waves. The maximum in $\sigma(\theta)$ near 30° , which is characteristic of the observed cross sections over a wide energy range, results from the corresponding peak in $H_3(\theta)$. We see that the behavior of the π^+ cross section at small angles is dominated by the one-pion-exchange term.⁸⁸ The fact that with the usual gauge this term vanishes at 0° depends on a delicate cancellation of all partial waves, and is more or less irrelevant.

3. S-Wave Resonance in A_{0+}

Evidence for an S -wave resonance in A_{0+} near 1560 MeV appears to be reasonably good in photoproduction data. There are four independent features of the data which indicate such a resonance. First is the asymmetry for linearly polarized photons $\Sigma(\theta)$ near 90° for π^+ as shown in Fig. 8. Part of the asymmetry near the high-energy end of the curve arises from an interference between the $B_{2-}(1519)$ resonance and the A_{0+} amplitude. If A_{0+} were primarily real in this region, the curve of $\Sigma(90^\circ)$ would pass through 0, becoming negative at an energy near the resonance. The observations seem to require a sizeable imaginary part of A_{0+} , and this indicates, although it does not require, a resonance in this amplitude. Secondly, the real part of A_{0+} for π^+ decreases rapidly in the region of 1560 MeV in a manner characteristic of the real part of a resonance. Third, the real part of A_{0+} for π^- production shows a similar behavior. Fourth, the steep angular dependence of the

⁸⁸ A similar point of view is expressed by L. Durand, III, Phys. Rev. Letters 19, 1345 (1967).

TABLE IX. Total helicity elements projected from the complete amplitudes for $\gamma n \rightarrow \pi^- p$, in units of $\mu b^{1/2}$. Imaginary parts, where nonzero, are given in parentheses.

k_{lab} (BeV)	0.200	0.250	0.300	0.350	0.400	0.460	0.505	0.600	0.700	0.790	0.875	0.965
W (BeV)	1.122	1.163	1.203	1.241	1.278	1.322	1.353	1.418	1.483	1.539	1.590	1.642
A_{0+}	-3.61 (-0.01)	-3.04 (-0.02)	-2.66 (-0.03)	-2.38 (-0.04)	-2.20 (-0.05)	-2.11 (-0.08)	-2.06 (-0.11)	-1.97 (-0.22)	-1.77 (-0.48)	-1.24 (-0.78)	-0.69 (-0.70)	-0.53 (-0.42)
A_{1-}	-0.58	-0.70	-0.70	-0.66	-0.57	-0.46 (-0.04)	-0.37 (-0.09)	-0.15 (-0.19)	-0.08 (-0.25)	-0.13 (-0.22)	-0.16 (-0.15)	-0.15 (-0.07)
A_{1+}	0.23 (0.05)	0.55 (0.27)	0.56 (0.83)	-0.08 (0.96)	-0.34 (0.61)	-0.35 (0.34)	-0.31 (0.24)	-0.24 (0.09)	-0.19 (-0.01)	-0.08 (-0.04)	0.02	0.10 (0.04)
B_{1+}	-1.90 (-0.12)	-2.57 (-0.67)	-2.42 (-2.00)	-0.77 (-2.34)	-0.11 (-1.47)	-0.11 (-0.81)	-0.20 (-0.54)	-0.34 (-0.20)	-0.43 (-0.02)	-0.48 (0.02)	-0.48 (0.01)	-0.47 (-0.03)
A_{2-}	0.14	0.13	0.13	0.16	0.20	0.24	0.28	0.34	0.40	0.36	0.36	0.36
B_{2-}	-0.30	-0.62	-0.83 (-0.00)	-0.96 (-0.00)	-1.07 (-0.01)	-1.16 (-0.02)	-1.22 (-0.04)	-1.34 (-0.15)	-1.27 (-0.77)	-0.20 (-0.79)	-0.03 (-0.28)	-0.13 (-0.17)
A_{2+}	-0.10	-0.13	-0.14	-0.14	-0.14	-0.14	-0.13	-0.13	-0.13	-0.13	-0.12	-0.12
B_{2+}	-0.10	-0.15	-0.17	-0.18	-0.18	-0.18 (0.00)	-0.17 (0.00)	-0.16 (0.00)	-0.13 (0.01)	-0.10 (0.03)	-0.08 (0.07)	-0.13 (0.14)
A_{3-}	0.03	0.05	0.06	0.06	0.06	0.05	0.04	0.03	0.02	0.01	-0.00	-0.01
B_{3-}	-0.05	-0.08	-0.09	-0.10	-0.10	-0.11 (-0.00)	-0.11 (-0.00)	-0.12 (-0.00)	-0.12 (-0.01)	-0.16 (-0.01)	-0.22 (-0.07)	-0.20 (-0.33)

creased from 0 to full strength over the energy region 1–2 BeV.

6. Helicities of Second and Third Resonances

The “second” and “third” resonances occur almost entirely in the B amplitudes, corresponding to initial helicity $\frac{3}{2}$. The argument that the corresponding A amplitudes are small is based on the fact that these resonances produce very little effect at 0° and 180° . A zero A -amplitude is equivalent to the following ratio of electric to magnetic multipole elements for these resonances:

$$\begin{aligned} \frac{3}{2}^-(1520): E_{2-}/M_{2-} &= 3, \\ \frac{5}{2}^+(1688): E_{3-}/M_{3-} &= 2. \end{aligned} \quad (33)$$

These ratios were first proposed by Beder⁹² in order to explain the very small cross section at 0° for π^0 photoproduction in the region of the second and third resonances. More sensitive evidence on the smallness of the A amplitudes comes from the behavior of the π^+ cross sections at 0° and 180° as functions of energy. As discussed by Ecklund and Walker,²⁷ small resonant A amplitudes would be expected to show up sensitively through interference with the smooth, predominantly real, nonresonant amplitudes at 0° and 180° ; the data show little or none of the expected characteristic behavior.

An attempt to understand the E/M ratios (33) on the basis of current commutation relations has been made by Bietti.⁹³

⁹² D. S. Beder, Nuovo Cimento 33, 94 (1964).

⁹³ A. Bietti, Phys. Rev. 142, 1258 (1966); 144, 1289 (1966).

7. $D_{5/2}$ Resonance

The resonant $D_{5/2}$ amplitude B_{2+} at 1652 MeV did not come from the present fitting procedure, but was taken from the polynomial fitting of π^+ data described by Ecklund and Walker.²⁷

8. Isospin Character of B_{2-} near $D_{3/2}(1519)$ Resonance

In the region near $W=1.520$ BeV, the imaginary parts of the resonant B_{2-} amplitudes for π^+ and π^0 do not seem to have the ratio $\sqrt{2}$ expected for an isospin- $\frac{1}{2}$ state. In fitting the data, the resonance has been put in a pure $I=\frac{1}{2}$ state, and the desired additional imaginary parts enter via the ΔB_{2-} terms as shown in Tables IV and V. Alternatively, a small $I=\frac{3}{2}$ B_{2-} resonance could be employed, but it would have no justification from the πN scattering analyses.

9. Polarization of Recoil Proton in $\gamma n \rightarrow \pi^- p$

A number of the helicity elements given for π^- in Table VI have appreciable imaginary parts. These were introduced solely to fit the single existing measurement⁷⁷ of polarization in the π^- reaction. One can fit the cross-section data alone rather easily without any imaginary parts in the added terms $\Delta A_{\perp\pm}$ and $\Delta B_{\perp\pm}$. Additional polarization data would obviously be useful.

10. π^+ Cross Sections at 0° and 180°

As pointed out above, the 0° and 180° cross sections for π^+ production show little of the sort of behavior that one might expect from resonances near 700 and 1025 MeV, and this fact forms the most sensitive basis for concluding that the initial helicity $\frac{1}{2}$ amplitudes A_{2-} and A_{3-} contribute little to the second and third resonances, respectively. Nevertheless, these cross

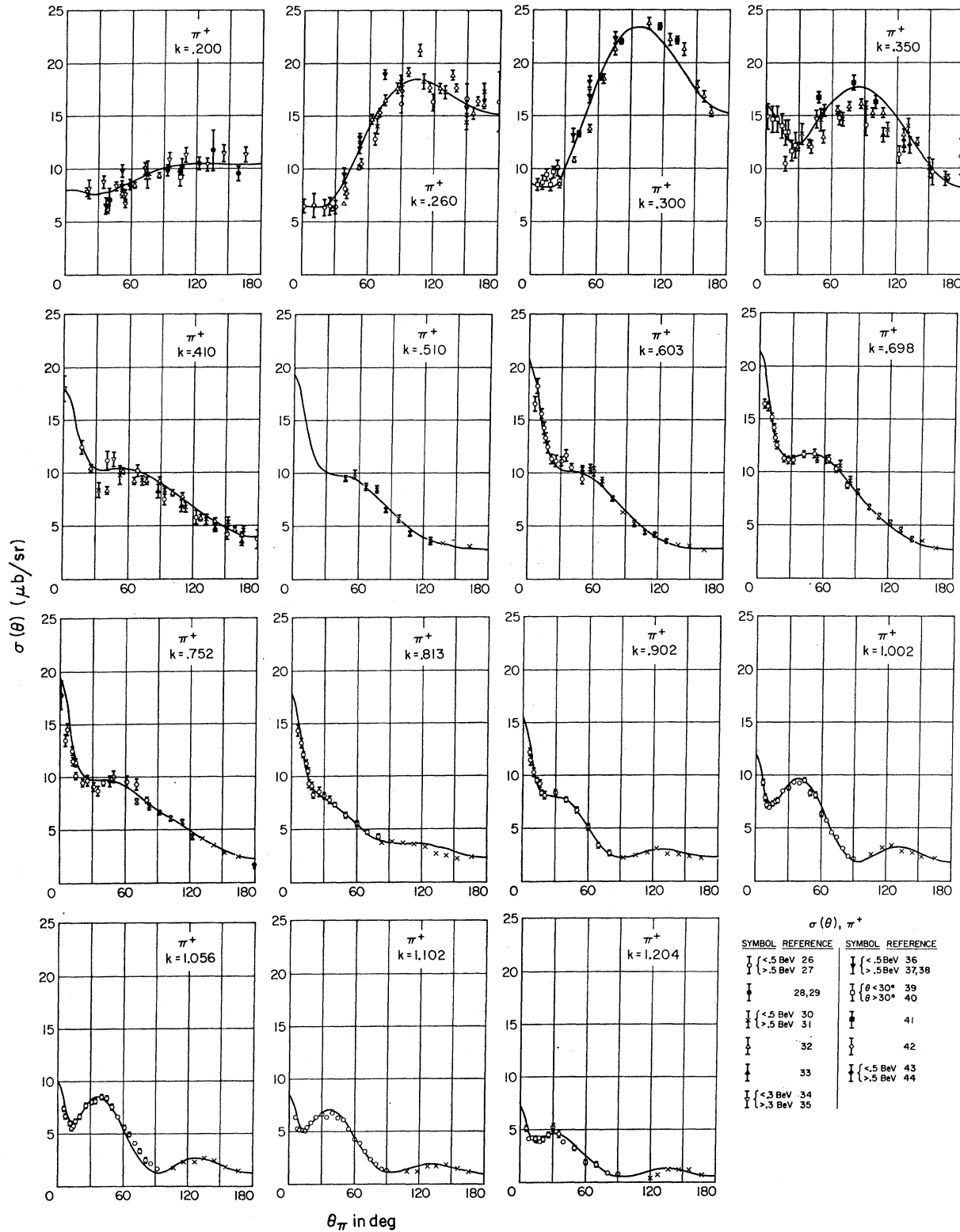


FIG. 4. Fits to differential cross sections for the reaction $\gamma p \rightarrow \pi^+ n$. Cross sections are given in units of $\mu\text{b}/\text{sr}$ as a function of the c.m. angle θ_π . The photon energy k is in units of BeV.

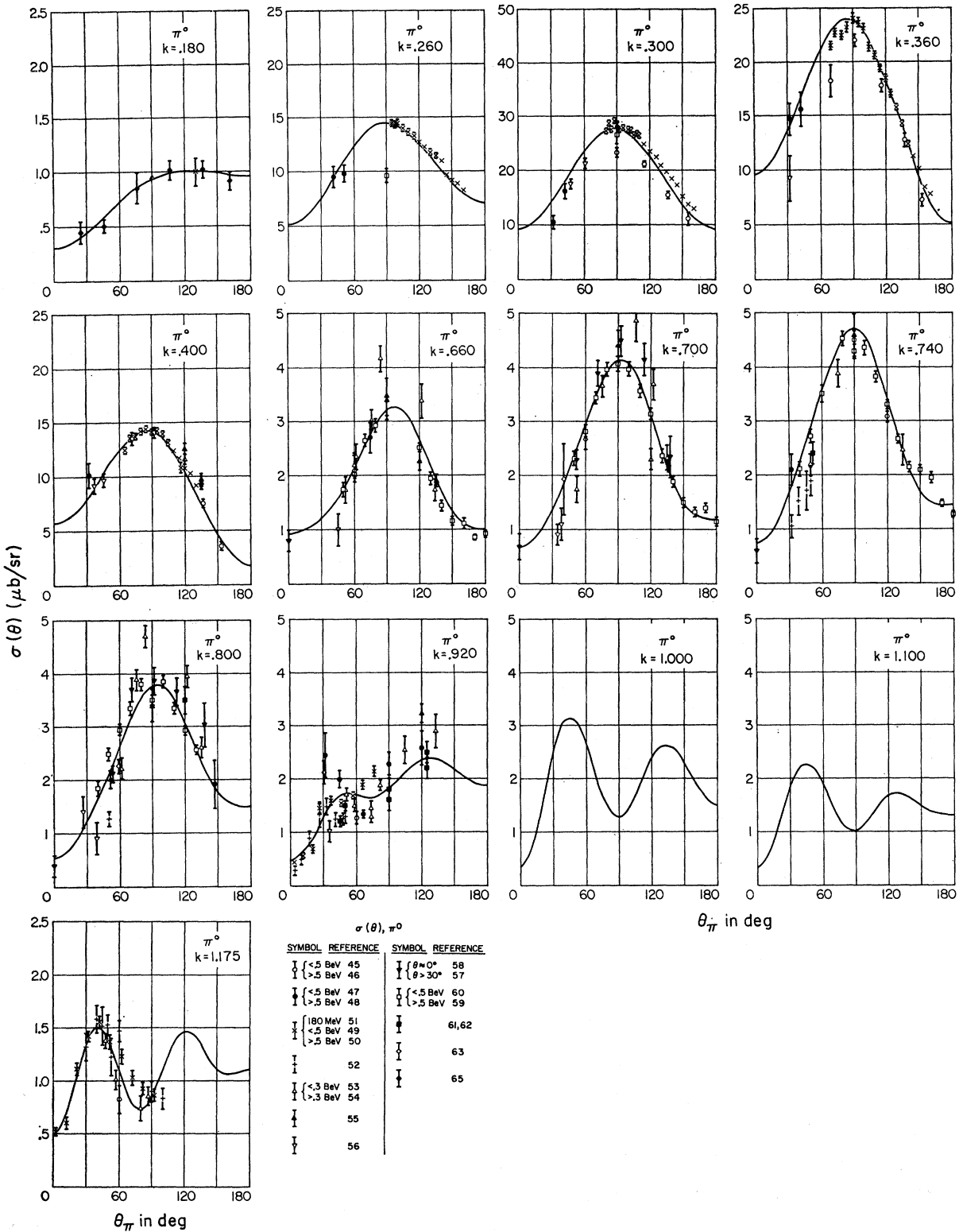


FIG. 5. Fits to differential cross sections for the reaction $\gamma p \rightarrow \pi^0 p$. The photon energy k is in units of BeV.

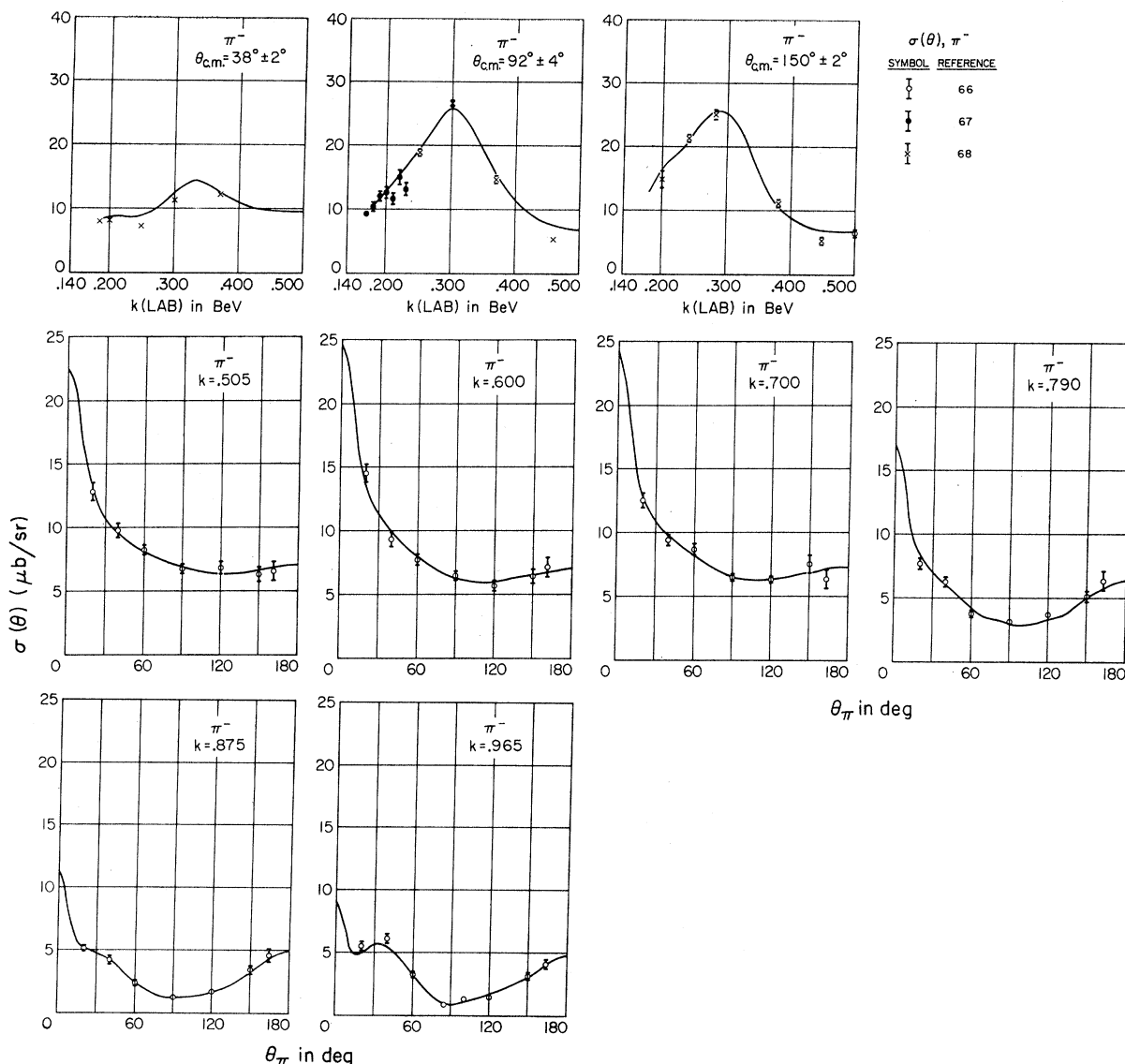


FIG. 6. Fits to energy distributions and angular distributions for the reaction $\gamma n \rightarrow \pi^- p$. The photon energy k is in units of BeV.

sections certainly have a peculiar behavior near the 700-MeV region as shown in Fig. 12. Since only one amplitude contributes at either 0° or 180° , the cross section may be written in the following simple form:

$$\sigma(\theta) = \frac{1}{2}(q/k) |V+B|^2 = \frac{1}{2}(q/k) (|V|^2 + |B|^2 + 2 \operatorname{Re}VB^*), \quad (34)$$

where V is the rapidly varying part of the amplitude, responsible for the peculiar energy dependence, and B is a background assumed to be smooth in energy. If we further assume that B is approximately real and correctly given by the present parametrization, and neglect the small term $|V|^2$, then

$$\sigma(\theta) \approx \frac{1}{2}(q/k) (|B|^2 + 2B \operatorname{Re}V). \quad (35)$$

Thus the deviation from the smooth background cross section will be

$$\Delta\sigma(\theta) \approx (q/k)B \operatorname{Re}V. \quad (36)$$

It seems reasonable to assign the part V to a single angular-momentum-parity state, a likely candidate being A_{0+} , for which the peculiar energy dependence might result from a cusplike behavior at the η threshold. With this assumption, we would have for the ratio of the deviations at 0° and 180°

$$\frac{\Delta\sigma(0^\circ)}{\Delta\sigma(180^\circ)} \approx -\frac{B(0^\circ)}{B(180^\circ)}, \quad (37)$$

so that the peculiar energy dependence at 0° would be the same as that at 180° except for a factor of approxi-

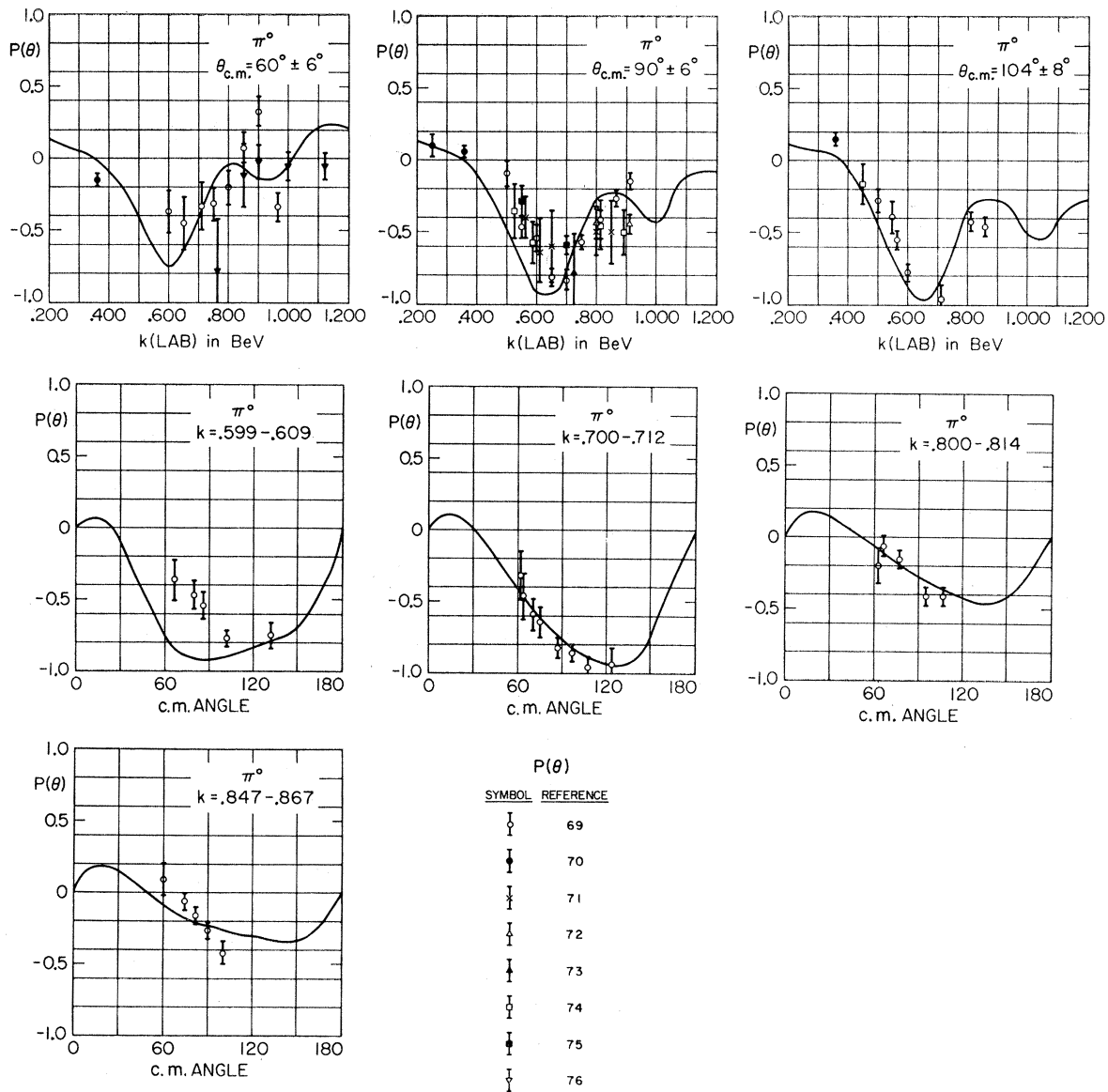


FIG. 7. Fits to some of the data on polarization of the recoil proton in the reaction $\gamma p \rightarrow \pi^0 p$. The photon energy k is in units of BeV.

mately -3 coming from the relative background amplitudes and the sign of V resulting from A_{0+} . This expectation is tested in Fig. 12, where smooth dashed curves are drawn to represent the cross sections resulting from the background B alone, the solid curve for $\sigma(180^\circ)$ is drawn through the data of Hand and Schaerf, and the solid curve at 0° is obtained from the curves at 180° by applying the above arguments. The solid curve for 0° fits the data well in some respects and poorly in others, so that the result is not as conclusive as one would like. Nevertheless, if the V part of the amplitude had been assumed to be the P wave A_{1-} , then the difference between the solid curve and the dashed curve at 0° would have had the opposite sign and the agreement

with the data would have been rather bad. If we conclude that the rapidly varying part of the amplitude is most likely A_{0+} and that the peculiar energy dependence is associated with the η threshold, then we may conclude that η photoproduction occurs strongly near threshold in an S state, in agreement with more direct evidence from the η photoproduction reaction.

11. Isoscalar and Isovector Photons

The isospin- $\frac{1}{2}$ states, including most of the resonances of Table III, can be produced by isoscalar or isovector photons. These may be distinguished by comparing the π^- and the π^+ (or π^0) parameters, using relations (29).

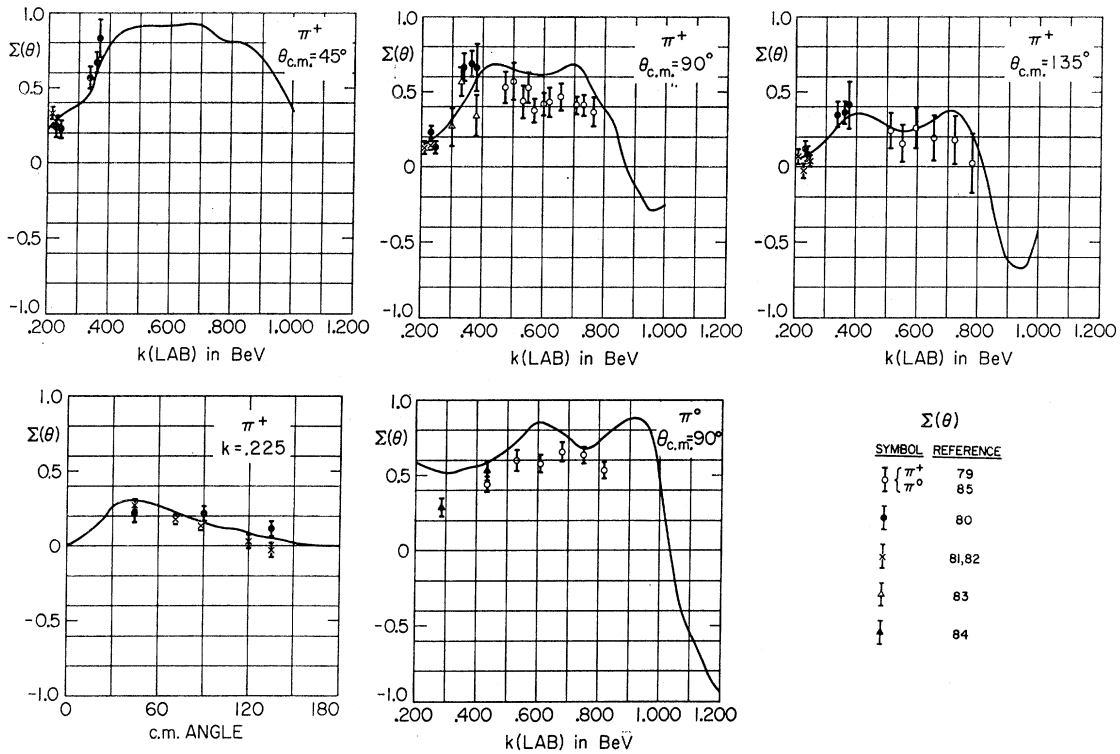


FIG. 8. Fits to data on the asymmetry from linearly polarized photons for both the π^+ and π^0 reactions. The photon energy k is in units of BeV.

From the resonant amplitudes in Table III, it may be seen that the most significant and well-determined resonances, B_{2-} , B_{3-} , and A_{0+} , are excited primarily

by isovector photons, the isoscalar parts being small. Additional data on the π^- reaction will be helpful in improving this isospin decomposition.

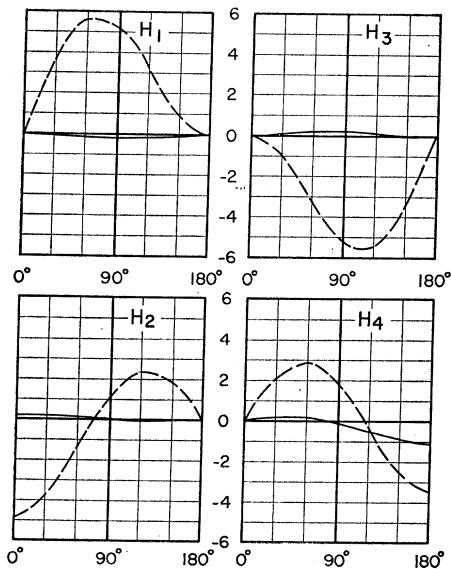


FIG. 9. Helicity amplitudes $H_n(\theta)$ for $\gamma p \rightarrow \pi^0 p$ at $k_{lab} = 350$ MeV. The real parts are shown by solid curves, the imaginary parts by dashed curves.

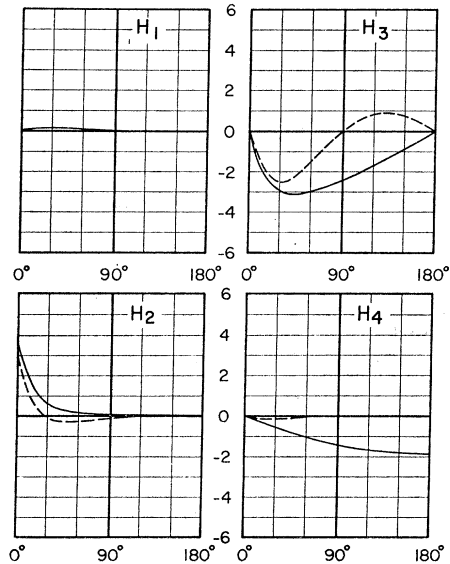
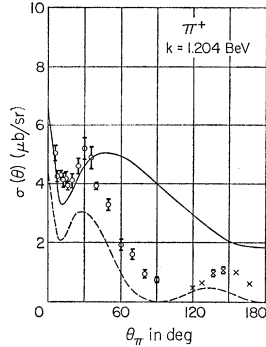


FIG. 10. Helicity amplitudes $H_n(\theta)$ corresponding to the electric Born approximation for $\gamma p \rightarrow \pi^+ n$ at $k_{lab} = 1.2$ BeV. The solid curves are the full electric Born approximation; the dashed curves are the result of subtracting the $j = \frac{1}{2}$ and $j = \frac{3}{2}$ components.

FIG. 11. Differential cross sections for $\gamma p \rightarrow \pi^+ n$ at $k_{\text{lab}} = 1.2$ BeV resulting from the helicity amplitudes of Fig. 10. The solid curve is the full electric Born approximation; the dashed curve is the result of subtracting the $j = \frac{1}{2}$ and $j = \frac{3}{2}$ components. Note how the dashed curve shows the qualitative features of the data.



12. Comparison with Dispersion Theory Results at Low Energies

As pointed out in the Introduction, the main emphasis in the present work was in the energy region above 500 MeV. The low-energy region was included, nevertheless, in order to make use of continuity requirements for the parameters, and also to see how the method would work there. It is of interest in this connection to note how the parameters obtained compare with those calculated from dispersion theory. For this comparison I shall use the dispersion theory calculations of Berends, Donachie, and Weaver,¹⁷ denoted hereafter by BDW.

A. π^+ Parameters

The parameters found for π^+ photoproduction agree well, in general, with BDW. My values of $\text{Re}B_{1+}$ are 0.05–0.20 $\mu\text{b}^{1/2}$ more negative, a minor difference for the dominant resonant state. The values of $\text{Im}A_{0+}$ differ by as much as 0.14 $\mu\text{b}^{1/2}$, because I have not forced the phases to have the proper values except where this would make a sizeable difference. At the lowest energies,

differences occur in A_{1-} , A_{1+} , and B_{2-} because my contributions $\Delta A_{1\pm}$ and ΔB_{2-} are kept constant, whereas the BDW values vary with energy. These differences produce very little effect on the resulting fits, and the BDW values are probably to be preferred. Above 400 MeV, the BDW fits are poor.

B. π^0 Parameters

Several of the parameters for $\gamma p \rightarrow \pi^0 p$ differ appreciably from those of BDW. The BDW values of $\text{Re}A_{1-}$ are 0.4–0.5 $\mu\text{b}^{1/2}$ more negative than mine throughout the low-energy region. My $\text{Re}A_{1+}$ is more positive below 300 MeV by as much as 0.3 $\mu\text{b}^{1/2}$ and is more negative above 450 MeV. In these regions the BDW fits are not as good. The difference in $\text{Re}B_{1+}$ varies from 0.2 to 0.7 $\mu\text{b}^{1/2}$ as k varies from 200 to 500 MeV, my values being more negative. As a result, the cross sections of BDW are too low at energies below the resonance and too high at energies above the resonance. The values of B_{2-} differ at energies above 350 or 400 MeV. My values are not required by the data in this energy region; they result from tying on smoothly to the parameters desired at higher energies.

C. π^- Parameters

Several parameters for π^- photoproduction differ from BDW by as much as 0.2 $\mu\text{b}^{1/2}$. However, the major difference occurs in A_{1-} ; the difference in $\text{Re}A_{1-}$ grows from 0.2 to 1.5 $\mu\text{b}^{1/2}$ as k goes from 200 to 500 MeV, the BDW values being more negative. However, the BDW fits become poor above 350 MeV, and are extremely bad near 500 MeV, so that a more detailed comparison of the π^- parameters does not seem warranted.

VII. NEED FOR ADDITIONAL DATA

The simple model employed in this analysis is surprisingly successful in describing the photopion data, within their present limitations and uncertainties. The “solution,” or parametrization, is certainly not unique, but the possibility of finding other, markedly different, solutions has not been carefully investigated. Although some of the parameters appear to be well determined by the data, others remain very uncertain, and it is not easy to present quantitative information on these uncertainties, for example, in the form of “errors.”

The above situation can be greatly improved by the accumulation of more data, particularly “complete sets” of data including cross sections, recoil-nucleon polarizations, polarized photon asymmetries, polarized-target data, etc. As seen by the formulas of Sec. III, each of these quantities is a (different) quadratic form in the helicity amplitudes $H_n(\theta)$ and each is *a priori* equally valuable in fixing the parameters.

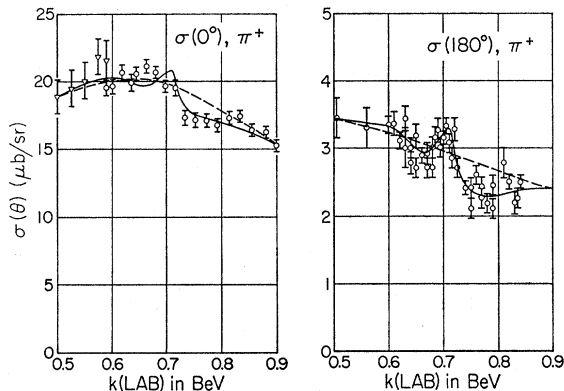


FIG. 12. Cross sections at 0° and 180° for $\gamma p \rightarrow \pi^+ n$. The 0° data are from Ecklund and Walker (Ref. 27) and the 180° data are those of Hand and Schaerf (Ref. 37) and Schaerf (Ref. 38). The dashed curves are hand-drawn smooth curves which connect smoothly to data outside this energy region. The solid curve at 180° is a hand-drawn fit to the data. The solid curve at 0° is the result of adding to the dashed curve three times the difference between the solid and dashed curves for 180° at the same energy.

If differential cross sections alone are available, the fitting is easy and certainly not unique. If two types of data exist over a reasonable range of energy and angle, the fitting becomes more difficult and the parameters

less uncertain. With more complete sets of data in the future, we may expect a considerable improvement in the situation concerning uniqueness and accuracy of the parameter determination.

Relations between Electron and Proton Excitation of N^* Resonances†

ALLEN RUBENSTEIN

Institute of Theoretical Physics, Department of Physics, Stanford University, Stanford, California 94305

(Received 13 January 1969)

We have taken various theories which relate the elastic electromagnetic form factors of the proton to the proton-proton scattering amplitude and, after briefly reviewing their content, have extended them in turn to diffractive excitation processes. We consider only very high-energy scattering $s \gg m^2, M^2$, where m (M) is the proton (resonance) mass. For large momentum transfer we find $X = G_E^{-2}(t) (|f_e|^2 + a|f_i|^2/|t|) m/M + O(1/s)$, where X is the ratio of $d\sigma/dt$ for $p+p \rightarrow p+N$ to that for $p+p \rightarrow p+p$, and the f 's are the standard inelastic electromagnetic form factors. $a = (2J+1)/J$. For small momentum transfer we employ both an additive quark model and an eikonal scattering model. In both models a direct connection is found between X and the electromagnetic form factors. The comparison of these theories with available data is very encouraging.

I. INTRODUCTION

AT very high energy, photon-hadron and hadron-hadron collisions become very similar, the photon in fact behaving as a vector meson (ρ^0, ω, φ). It is then natural to expect that there exists a relationship between the two interactions that have had the greatest experimental attention at high energy, electron-proton and proton-proton scattering. Such relations have been found for the elastic channel of these two reactions and explained from several points of view.¹⁻⁴ We shall examine the situation for the quasielastic channel.

The idea of Wu and Yang¹ that the most important effect seen in high-energy scattering at large momentum transfer is the inability of the particles to resist breakup (i.e., excitation) when hit very hard, and that this idea need not take into account specific details of the interactions producing the large momentum transfer, leads to relations between different scattering processes such as

$$\frac{d\sigma}{dt} / \left(\frac{d\sigma}{dt} \right)_{t=0} = G_E^4(t), \quad (1)$$

where $d\sigma/dt$ is the partial cross section for proton-proton elastic scattering, and G_E is the elastic electric form

factor of the proton. Figures 1 and 2 show the data in support of Eq. (1). Other investigators have interpreted Eq. (1) as an asymptotic limit² ($s \rightarrow \infty$), suggested an interaction mechanism and found excellent support in the experimental data, or have derived it from com-

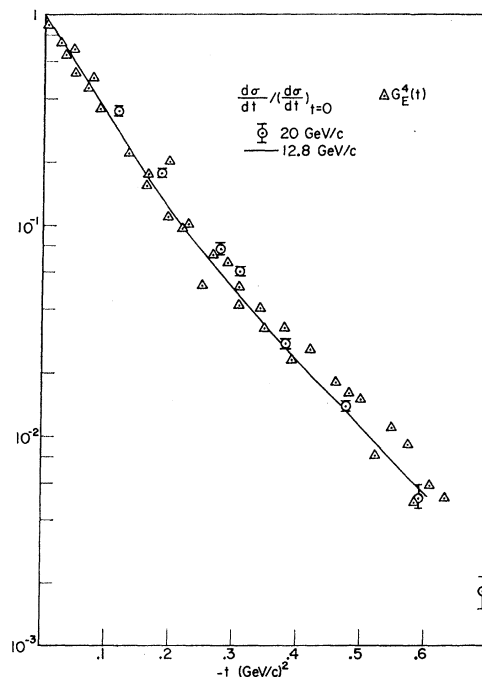


Fig. 1. Comparison of $G^4(t)$ with elastic proton-proton scattering data at small momentum transfer. After Ref. 3 and R. C. Arnold and S. Fenster, 1968 CERN Topical Conference, Vol. II, p. 20 (unpublished).

† Research sponsored by the Air Force Office of Scientific Research, Office of Aerospace Research, U. S. Air Force, under AFOSR Contract No. F44620-68-C-0075.

¹ Tai Tsen Wu and C. N. Yang, Phys. Rev. **137**, B708 (1965).

² H. D. I. Abarbanel, S. D. Drell, and F. J. Gilman, Phys. Rev. Letters **20**, 280 (1968); Phys. Rev. **177**, 2458 (1969).

³ L. Van Hove, in *Particle Interactions at High Energies*, edited by T. W. Priest and L. J. Vick (Plenum Press, Inc., New York, 1967), p. 96.

⁴ T. T. Chou and C. N. Yang, Phys. Rev. **170**, 1591 (1968); Loyal Durand and Richard Lipps, Phys. Rev. Letters **20**, 637 (1968).